Optimization of Critical Drive Head of Hydraulic Ram Pump by Analyzing Different Design Parameters, Performance and Cost Implications

Submitted By

Nifat Mouddit Nizhum

200011119

Fardin Hasnine Choudhury

200012125

Mueen Shabib Al Forkan

200012134

Supervised By

Dr. Md Abu Shaid Sujon

Co-Supervised By

Dr. M Monjurul Ehsan

A Thesis submitted in partial fulfillment of the requirement for the degree of Bachelor of Science in Mechanical Engineering

Department of Mechanical and Production Engineering (MPE)

Islamic University of Technology (IUT)

September, 2025

Candidate's Declaration

This is to certify that the work presented in this thesis, titled, "Optimization of Critical Drive Head of Hydraulic Ram Pump by Analyzing Different Design Parameters, Performance and Cost Implications", is the outcome of the investigation and research carried out by me under the supervision of Dr. Md Abu Shaid Sujon, Assistant Professor, Department of Mechanical and Production Engineering, Islamic University of Technology.

It is also declared that neither this thesis nor any part of it has been submitted elsewhere for the award of any degree or diploma.

Nifat Mouddit Nizhum
Student No: 200011119

Fardin Hasnine Choudhury
Student No: 200012125

Mueen Shabib Al Forkan
Student No: 200012134

Recommendation of the Thesis Supervisors

The thesis titled "Optimization of Critical Drive Head of Hydraulic Ram Pump by Analyzing Different Design Parameters, Performance and Cost Implications" submitted by Nifat Mouddit Nizhum, Student No: 200011119, Fardin Hasnine Chouhdury, Student No: 200012125 and Mueen Shabib Al Forkan, Student No: 200012134 has been accepted as satisfactory in partial fulfillment of the requirements for the degree of B Sc. in Mechanical Engineering **on 29th September, 2025.**

1.

(Supervisor)

Dr. Md. Abu Shaid Sujon
Assistant Professor
MPE Dept., IUT, Board Bazar, Gazipur-1704, Bangladesh.

CO-PO Mapping of ME 4800 -Theis and Project

COs	Course Outcomes (CO) Statement	(PO)	Addressed by	
CO1	Discover and Locate research problems and illustrate them via figures/tables or projections/ideas through field visit and literature review and determine/Setting aim and objectives of the project/work/research in specific, measurable, achievable, realistic and timeframe manner.	**PO2 Problem analysis**	Thesis Book	√
			Performance by research	√
			Presentation and soft skill	√
CO2	Design research solutions of the problems towards achieving the objectives and its application. Design systems, components or processes that meets related needs in the field of mechanical engineering	**PO3 Design/development of solutions**	Thesis Book	√
			Performance by research	√
			Presentation and soft skill	√
CO3	Review, debate, compare and contrast the relevant literature contents. Relevance of this research/study. Methods, tools, and techniques used by past researchers and justification of use of them in this work.	**PO4 Investigation**	Thesis Book	√
			Performance by research	√
			Presentation and soft skill	√
CO4	Analyse data and exhibit results using tables, diagrams, graphs with their interpretation. Investigate the designed solutions to solve the problems through case study/survey study/experimentation/simulation using modern tools and techniques.	**PO5 Modern tool usage**	Thesis Book	√
			Performance by research	√
			Presentation and soft skill	√
CO5	Apply moral values and research/professional ethics throughout the work, and justify genuine referencing on sources, and demonstration of own contribution.	**PO8 Ethics**	Thesis Book	√
			Performance by research	√
			Presentation and soft skill	√
CO6	Perform own self and manage group activities from the beginning to the end of the research/work as a quality work.	**PO9 Individual work and teamwork**	Thesis Book	√
			Performance by research	√
			Presentation and soft skill	√
CO7	Compile and arrange the work outputs, write the report/thesis, a sample journal paper, and present the work to wider audience using modern communication tools and techniques.	**PO10 Communication**	Thesis Book	√
			Performance by research	√
			Presentation and soft skill	√
CO8	Recognize the necessity of life-long learning in career development in dynamic real-world situations from the experience of completing this project.	**PO12 Life-long learning**	Thesis Book	√
			Performance by research	√
			Presentation and soft skill	√

Student Name /ID:

1……………………………………..

2. ……………………………………..

3. ……………………………………..

Signature of the Supervisor:

…………………………

Name of the Supervisor:

……………………………..

K-P-A Mapping of ME 4800 -Theis and Project

COs	POs	Related Ks								Related Ps							Related As				
		K1	K2	K3	K4	K5	K6	K7	K8	P1	P2	P3	P4	P5	P6	P7	A1	A2	A3	A4	A5
CO1	PO2	√	√	√	√					√											
CO2	PO3					√				√	√	√				√	√	√	√		
CO3	PO4								√	√	√	√					√	√			
CO4	PO5						√			√				√							
CO5	PO8							√													
CO6	PO9																				
CO7	PO10																				
CO8	PO12																				

Student Name /ID:

1……………………………………..

2. ……………………………………..

3. ……………………………………..

Signature of the Supervisor:

…………………………

Name of the Supervisor:

……………………………..

List of Sustainable Development Goals (SDGs) Addressed in this Project

SDG No.	Goals	Targets	Relevance to the Thesis	Remarks
1	No Poverty	1.1 Eradicate extreme poverty (people living on less than $1.25/day).		
		1.2 Reduce poverty in all its forms by at least half.		
		1.3 Implement nationally appropriate social protection systems.		
		1.4 Ensure equal rights to economic resources, services, property, inheritance, technology, and financial services.		
		1.5 Build resilience of the poor and reduce exposure to climate-related and other shocks.		
		1.a Mobilize resources to end poverty.		
		1.b Create pro-poor policy frameworks.		
2	Zero Hunger	2.1 End hunger and ensure access to safe, nutritious food year-round.		
		2.2 End all forms of malnutrition.		
		2.3 Double agricultural productivity and incomes of small-scale producers.		
		2.4 Ensure sustainable food production systems and resilient agricultural practices.		
		2.5 Maintain genetic diversity of seeds, plants, and animals.		
		2.a Increase investment in rural infrastructure, research, and technology.		
		2.b Correct and prevent trade restrictions/distortions in global food markets.		
		2.c Adopt measures to ensure proper functioning of food commodity markets.		
3	Good Health and Well-Being	3.1 Reduce global maternal mortality ratio.		
		3.2 End preventable deaths of newborns and under-5 children.		
		3.3 End epidemics of AIDS, tuberculosis, malaria, and neglected tropical diseases.		
		3.4 Reduce premature mortality from NCDs and promote mental health.		
		3.5 Strengthen prevention and treatment of substance abuse.		

		3.6 Halve global deaths/injuries from road traffic accidents.		
		3.7 Ensure universal access to sexual and reproductive healthcare.		
		3.8 Achieve universal health coverage.		
		3.9 Reduce deaths from hazardous chemicals, pollution, and contamination.		
		3.a Strengthen tobacco control (WHO FCTC).		
		3.b Support R&D of vaccines and medicines.		
		3.c Increase health financing and workforce.		
		3.d Strengthen capacity for early warning and risk management.		
4	Quality Education	4.1 Ensure all complete free, equitable, quality primary and secondary education.		
		4.2 Ensure access to quality early childhood development and pre-primary education.		
		4.3 Ensure equal access to affordable technical, vocational, and higher education.		
		4.4 Increase skills for employment and entrepreneurship.		
		4.5 Eliminate gender disparities in education.		
		4.6 Ensure literacy and numeracy for youth and adults.		
		4.7 Ensure learners acquire knowledge/skills for sustainable development.	√	Research contributes to academic knowledge in green technology.
		4.a Build and upgrade education facilities that are inclusive and safe.		
		4.b Expand scholarships for developing countries.		
		4.c Increase supply of qualified teachers.		
5	Gender Equality	5.1 End all forms of discrimination against women and girls.		
		5.2 Eliminate violence against women and girls.		
		5.3 Eliminate harmful practices (child, early, forced marriage, FGM).		
		5.4 Recognize and value unpaid care and domestic work.		
		5.5 Ensure women’s participation in leadership and decision-making.		
		5.6 Ensure universal access to reproductive health and rights.		

		5.a Undertake reforms to give women equal rights to resources.		
		5.b Enhance use of enabling technology to empower women.		
		5.c Adopt and strengthen policies and laws for gender equality.		
6	Clean Water and Sanitation	6.1 Achieve universal and equitable access to safe drinking water.	√	HRP provides clean water in rural/agricultural areas without electricity.
		6.2 Achieve access to adequate sanitation and hygiene.		
		6.3 Improve water quality by reducing pollution.		
		6.4 Increase water-use efficiency and sustainable withdrawals.	√	Pump reuses flowing water efficiently using water hammer effect.
		6.5 Implement integrated water resources management.	√	Promotes decentralized, low-cost water management.
		6.6 Protect and restore water-related ecosystems.		
		6.a Expand international cooperation in water and sanitation.		
		6.b Support participation of local communities.		
7	Affordable and Clean Energy	7.1 Ensure universal access to affordable, reliable, modern energy services.	√	Works without fuel/electricity—affordable for rural communities.
		7.2 Increase substantially the share of renewable energy.		
		7.3 Double global rate of improvement in energy efficiency.	√	HRP operates on renewable gravitational energy with no external input.
		7.a Enhance international cooperation on clean energy research/technology.		
		7.b Expand infrastructure and upgrade technology for sustainable energy.		
8	Decent Work and Economic Growth	8.1 Sustain per capita economic growth.		
		8.2 Achieve higher levels of productivity through diversification, tech, and innovation.	√	Supports rural economies by enabling efficient farming.
		8.3 Promote policies for decent job creation and entrepreneurship.		

		8.4 Improve resource efficiency in production and consumption.	√	Balances material cost with performance efficiency.
		8.5 Achieve full and productive employment for all.		
		8.6 Substantially reduce youth not in employment/education/training.		
		8.7 Eradicate forced labour, modern slavery, and child labour.		
		8.8 Protect labour rights and safe working environments.		
		8.9 Promote sustainable tourism.		
		8.a Increase aid for trade support.		
		8.b Develop a global youth employment strategy.		
9	Industry, Innovation, and Infrastructure	9.1 Develop quality, reliable, sustainable infrastructure.	√	HRP offers sustainable water infrastructure for rural areas.
		9.2 Promote inclusive and sustainable industrialization.		
		9.3 Increase access of SMEs to financial services and integration into value chains.		
		9.4 Upgrade infrastructure for sustainability and resource efficiency.	√	Design optimization balances cost and efficiency.
		9.5 Enhance scientific research and technology development.	√	Our thesis uses ANN–RSM–XGBoost models for pump optimization.
		9.a Facilitate sustainable infrastructure in developing countries.		
		9.b Support domestic tech development and value addition.		
		9.c Increase access to ICT and internet.		
10	Reduced Inequalities	10.1 Achieve income growth of bottom 40%.		
		10.2 Empower and promote inclusion regardless of status.		
		10.3 Ensure equal opportunity and reduce inequalities of outcome.		
		10.4 Adopt policies for fiscal, wage, and social protection equality.		
		10.5 Improve regulation of global financial markets.		
		10.6 Ensure enhanced representation in global institutions.		
		10.7 Facilitate safe, regular, and responsible migration.		

		10.a Implement special treatment for developing countries.		
		10.b Encourage development assistance and investment in least developed areas.		
		10.c Reduce remittance costs.		
11	Sustainable Cities and Communities	11.1 Ensure access to adequate, safe, and affordable housing.		
		11.2 Provide sustainable transport systems.		
		11.3 Enhance inclusive urbanization and capacity for planning.		
		11.4 Protect cultural and natural heritage.		
		11.5 Reduce disaster impact and losses.		
		11.6 Reduce environmental impact of cities (air quality, waste).		
		11.7 Provide access to safe, inclusive green/public spaces.		
		11.a Support positive links between urban, peri-urban, rural.		
		11.b Increase disaster risk reduction strategies.		
		11.c Support least developed countries in sustainable building.		
12	Responsible Consumption and Production	12.1 Implement 10-Year Framework on sustainable consumption/production.		
		12.2 Achieve sustainable management and use of resources.	√	HRP reduces dependency on fossil fuel-driven pumps.
		12.3 Halve per capita global food waste.		
		12.4 Manage chemicals and waste sustainably.		
		12.5 Substantially reduce waste generation.	√	Efficient water use minimizes water and energy waste.
		12.6 Encourage companies to adopt sustainable practices.		
		12.7 Promote sustainable public procurement.		
		12.8 Ensure people have relevant information for sustainable development.		
		12.a Support developing countries' scientific and technological capacity.		
		12.b Develop tools to monitor sustainable tourism impacts.		
		12.c Rationalize inefficient fossil-fuel subsidies.		

13	Climate Action	13.1 Strengthen resilience and adaptive capacity to climate-related hazards.	√	HRP supports water access during seasonal variations.
		13.2 Integrate climate measures into national policies.	√	Renewable pump technology aligns with green energy policies.
		13.3 Improve education and awareness on climate change.		
		13.a Implement UNFCCC commitments (mobilize $100 billion annually).		
		13.b Promote mechanisms for capacity-building in least developed countries.		
14	Life Below Water	14.1 Reduce marine pollution.		
		14.2 Sustainably manage and protect marine ecosystems.		
		14.3 Minimize and address ocean acidification.		
		14.4 Regulate harvesting and end overfishing.		
		14.5 Conserve at least 10% of coastal and marine areas.		
		14.6 Prohibit harmful fisheries subsidies.		
		14.7 Increase economic benefits from sustainable marine resources.		
		14.a Increase scientific knowledge and marine technology transfer.		
		14.b Provide access for small-scale artisanal fishers.		
		14.c Implement international law for oceans.		
15	Life on Land	15.1 Conserve terrestrial and freshwater ecosystems.	√	Reduces over-extraction of groundwater, protecting ecosystems.
		15.2 Promote sustainable management of forests.		
		15.3 Combat desertification and restore degraded land.		
		15.4 Ensure conservation of mountain ecosystems.		
		15.5 Take urgent action to reduce biodiversity loss.		
		15.6 Promote fair benefit-sharing from genetic resources.		
		15.7 End poaching and trafficking of protected species.		
		15.8 Prevent introduction of invasive alien species.		

		15.9 Integrate ecosystem values into policies/planning.		
		15.a Mobilize resources for biodiversity.		
		15.b Finance sustainable forest management.		
		15.c Support local communities for forest and wildlife.		
16	Peace, Justice and Strong Institutions	16.1 Reduce violence and related death rates.		
		16.2 End abuse, trafficking, and violence against children.		
		16.3 Promote rules of law and equal access to justice.		
		16.4 Reduce illicit financial/arms flows, organized crime.		
		16.5 Reduce corruption and bribery.		
		16.6 Develop effective, accountable institutions.		
		16.7 Ensure inclusive, participatory decision-making.		
		16.8 Broaden participation of developing countries in global governance.		
		16.9 Provide legal identity for all (including birth registration).		
		16.10 Ensure access to information and protect freedoms.		
		16.a Strengthen national institutions for prevention of violence.		
		16.b Promote/enforce non-discriminatory laws and policies.		
17	Partnerships for the Goals	17.1 Strengthen domestic resource mobilization.		
		17.2 Developed countries to implement ODA commitments.		
		17.3 Mobilize additional financial resources.		
		17.4 Assist developing countries with debt sustainability.		
		17.5 Invest in least developed countries.		
		17.6 Enhance access to science, technology, innovation.	√	Promotes knowledge-sharing of low-cost sustainable tech.
		17.7 Promote environmentally sound technologies.	√	HRP is an eco-friendly, zero-emission technology.
		17.8 Fully operationalize technology bank for LDCs.		

		17.9 Enhance international support for capacity-building.		
		17.10 Promote a universal, rules-based trading system (WTO).		
		17.11 Increase exports of developing countries.		
		17.12 Timely implementation of duty-free, quota-free market access.		
		17.13 Enhance global macroeconomic stability.		
		17.14 Enhance policy coherence for sustainable development.		
		17.15 Respect national policy space.		
		17.16 Enhance global partnerships.		
		17.17 Encourage multi-stakeholder partnerships.		
		17.18 Enhance data capacity of developing countries.		
		17.19 Support capacity-building for sustainable development indicators.		

Acknowledgment

Bismillah Ir-Rahamn n-Ir Raheem

First of all, we are grateful to ALLAH (SWT), the most benign and compassionate, for granting us the power and capability to compose this dissertation. We want to thank our project supervisor, **Dr. Md. Abu Shaid Sujon**, Assistant Professor, IUT for his strong and patient support through unpredictable problems during the project and his precious advice whenever we faced difficulties. His benevolence, compassion, and effective oversight at work alleviated our stress in facing unforeseen challenges and enhanced our productivity in personal endeavors.

We would also like to express our deepest gratitude and acknowledgement to **Dr. Mohammad Monjurul Ehsan**, Professor, IUT for his unwavering support, invaluable guidance, and encouragement throughout the project.

We are thankful to **Dr. Md Hamidur Rahman**, Former Professor, IUT for his guidance in the initial days of our project. His prospective helped us greatly to concrete the idea and objectives of our project.

We would also like to thank **Md. Azazul Haque**, Graduate Research Assistant at Idaho State University for his tutorials in generating our results. Only for his supported, we could overcome the hardship that we faced during the fabrication process of our experimental setup.

We extend our gratitude to our family and friends for their unwavering support and encouragement. To our parents, for their unwavering love, faith in us, and steadfast support for our academic pursuits, and to our friends, for their patience and understanding during this arduous path.

Abstract

This study explores an experimental and theoretical investigation into the optimization of the performance of a Hydraulic Ram Pump (HRP) for sustainable water lifting applications in off-grid rural and agricultural settings. To assess the effects of different design parameters on its performance, a detailed parametric study is conducted. A benchtop experimental setup was devised to assess the impact of five critical design parameters, drive pipe length (78-242 inches), delivery head (48-152 inches), drive and delivery pipe diameters (0.75-1.25 inches), and air chamber volume (1.03-5.35 L) on pump performance. The critical drive head, which is the lowest supply head needed for the pump to work properly, turned out to be an important but little-studied factor that affects how well the pump works in different seasons and how much maintenance it requires. The experiments showed that the system had maximum efficiency when the L/D ratio was 260 with a 65-inch delivery head, and the critical drive head was 14.65 inches, generating 61.34% efficiency. For multi-objective optimization, a weighted ensemble model was made with Artificial Neural Networks (40%), XGBoost (40%), and RSM (20%) with 39 sets of experimental and 5000 synthetic sample best setups that maximized efficiency and delivery flow rate while minimizing critical drive head and total cost. The best configuration for Pareto optimization had 61.34% efficiency, a total cost of $232.27, a critical drive head of 13.6 inches, and a delivery flow rate of 2.23 L/min. Cost analysis showed that pipe parts make up the majority of system costs (50.5% to 65.9%), which shows the trade-off between efficiency and cost (r = -0.78). These results offer crucial design principles for the economical implementation of HRP in rural agricultural and off-grid water pumping contexts.

Keywords: Hydraulic ram pump; Sustainable water supply; Critical drive head; Water hammer effect; Cost analysis; Multi-objective optimization; Hybrid ensemble machine learning model.

Summary

Access to clean and reliable water is still a challenge for many rural communities, especially where electricity or fuel-powered pumps are costly or unavailable. To address this problem, we worked on a project involving a Hydraulic Ram Pump (HRP) – a simple water-lifting device that operates without electricity or fuel. It uses the natural energy of flowing water to lift part of that water to a higher level, making it an affordable and sustainable option for households and farmers.

In our thesis, we aimed to make the pump more efficient, cost-effective, and reliable**.** We carried out experiments to understand how different factors, such as water flow and pressure, affect its performance. To improve the design further, we also applied modern computer-based models to predict and optimize the pump's efficiency.

Through this work, we achieved several key outcomes: we developed a low-cost, eco-friendly pumping system suitable for rural use, improved its efficiency through design optimization, and demonstrated its potential to save water and reduce dependency on fossil-fuel-driven pumps. Most importantly, our project supports global sustainability efforts by aligning with the United Nations Sustainable Development Goals (SDGs), including clean water, clean energy, climate action, and poverty reduction.

This project shows that a simple and affordable technology can bring big benefits to communities, agriculture, and the environment. By combining teamwork, experiments, and modern tools, we have created a solution that is not only technically effective but also socially impactful**.**

Table of Contents

List of Figures

List of Tables

Nomenclatures and Symbols

Nomenclature

H_d	Drive head (inch)
H_D	Delivery head (inch)
H_C	Critical drive head (inch)
D_d	Drive pipe diameter (inch)
D_D	Delivery pipe diameter (inch)
L	Drive pipe length (inch)
V_A	Air chamber volume (L)
P_A	Air chamber pressure (mbar)
L/D	Drive pipe length-Drive pipe diameter ratio
h/L	Drive pipe length-Drive head ratio
D/d	Drive pipe diameter-Delivery pipe diameter ratio
h/H	Drive head-Delivery head ratio
η	Efficiency of the pump (%)
C_t	Total cost of the system ($)
Q_s	Drive pipe flow rate (L/min)
Q_d	Delivery pipe flow rate (L/min)
Q_w	Waste valve flow rate (L/min)
N	No. of beats per min
W	Weight of impulse valve (N)
s	Length stroke of impulse valve
f	Friction factor of the pipe
h_L	Total minor losses
RS	Total head loss factor to the waste valve
V	Velocity of water in the drive pipe
M	Total head loss factor (major) of both the drive pipe and waste valve
V_0	Threshold velocity at waste valve closure
A_v	Projected surface area of waste valve
γ	Specific weight of water
C_d	Drag coefficient
V_s	Average steady flow velocity
m	Flow ratio
V_{sp1}	Volume of total water supplied by drive pipe

V_{sp3}	Volume of total delivered water by delivery pipe
c	Wave celerity of a pressure wave in water
g	Gravitational acceleration
K_C	Composite modulus of elasticity of water and pipe
ρ	Density of water
K	Bulk modulus of water
K_L	Loss coefficient
E	Modulus of elasticity of the pipe material
t_p	Pipe thickness (mm)
h_r	Total head loss in the delivery head
HVD	Friction loss coefficient of the delivery valve
h_{max}	Maximum theoretical delivery head
V_3	Maximum flow velocity
N	Head loss factor of the drive pipe and delivery valve
t_1	Cycle duration during period A
t_2	Cycle duration during period B
t_3	Cycle duration during period C
t_4	Cycle duration during period D
T	Duration of one complete cycle
r	Pearson correlation coefficient
R^2	Coefficient of determination

Abbreviations

HRP	Hydraulic Ram Pump
RSM	Response surface regression
ANN	Artificial Neural Networks
XGBoost	Extreme Gradient Boosting
MAPE	Mean absolute percentage error
MAE	Mean absolute error
RMSE	Root mean square error
NGO	Non-government organization

Chapter 1: Introduction

1.1 Background of the Study

In this modern era, the world is shifting towards sustainable and renewable energy sources. Traditional energy sources are dwindling day by day, which negatively impacts the environment. Water remains a fundamental necessity for humans [1]. Water is essential for agriculture and industrial processes. Extracting and using water from a resource is a challenging and costly process in rural areas [2]. Generally, centrifugal pumps are used to extract groundwater. However, the fuel consumption costs are logistically and financially unfeasible. In this scenario, Hydraulic ram pump (HRP) gives water elevation without any fuel consumption and supplies water in a very sustainable and cost-effective way. HRP uses water hammer effect to lift water to an elevation from a lower height. The kinetic energy from continuous water flow pumps a portion of the water to a higher delivery point [3]. The HRP works in a cycle without electricity and fuel, which makes it an alternative and attractive solution for water sources in hilly and underdeveloped areas [4]. HRP was first introduced in the 18th century but due to the industrial revolution, it remained underutilized.

The principle behind the HRP, known as water hammer, has been known since ancient times. The HRP itself was invented in the late 18th century by French inventor Joseph Michel Montgolfier in 1796 [5]. This self-operating pump concept was first introduced in England in 1797. Industrialists like James Watt and Mathew Boulton patented their own versions of the ram pump, which facilitated further development and commercialization of this system. Due to its affordability and low maintenance needs, rural and village communities in North America and Europe began using HRPs in the 19th and early 20th centuries. A UK based company, Green and Carter, started manufacturing the pumps commercially and produced effective models [6]. Several non-governmental organizations (NGO'S) promoted the credibility and effectiveness of such pumps in underdeveloped regions of Africa, Asia, and Latin America [7]. Modern developments are focusing on optimizing design parameters, configuration, working mechanism, with implementation of advanced material characteristics to enhance efficiency at a possible low cost.

1.2 Advancement in Hydraulic Ram Pump Performance Parameters

The performance and maintenance of HRPs are critically dependent on various performance parameters, such as the length of the drive pipe and delivery pipe, the geometry and design of the waste valve, the volume of the air chamber, and the configuration setup. Current focus areas include the optimization of key parameters and the advancement of material properties to minimize preventive maintenance requirements. Computational Fluid Dynamics (CFD) and numerical studies are being employed to improve the drive to delivery ratio and to reduce head losses and energy dissipation. Experimental research remains more effective than sole reliance on numerical studies; the experimental results aid in creating models to predict and optimize pump performance prior to construction.

1.3 Problem Statement and Research Scope

The HRP system requires a minimum drive head to operate, though the earlier research had identified it none studied its impact on the other operating parameters or vice versa. As a critical parameter, the minimum supply or drive head is essential for the smooth operation of a pump. When installing the pump in a river or water reservoir, if the drive head is set below the water's critical level, the drive pipe won't have enough pressure to operate the pump effectively. So, based on its properties, we are redefining this parameter as Critical drive head. Water levels in rivers vary seasonally, so understanding the critical drive head is vital; without it, the pump may require seasonal maintenance, and pressure loss can prevent the waste valve from closing, disrupting the pump cycle. The critical drive head varies with different configurations. This study aims to establish the relationships among various design parameters and the critical drive head. As performance parameters improve, the manufacturing cost also increases. One of the primary objectives of HRP is to provide higher elevation head at a lower cost. A cost analysis, considering efficiency and performance, will offer guidelines for better pump layout design. Previous studies have shown that increasing the drive head and diameter enhances water flow and improves efficiency. However, increasing material dimensions leads to higher assembly costs. It is not optimal to escalate expenditure solely to achieve higher efficiency. To utilize HRP in rural areas for agriculture and other purposes, the cost and efficiency levels must be balanced optimally. The pump system should be designed to maximize efficiency while minimizing costs. Developing a mathematical model to predict pump performance based on various parameters and dimension data that will facilitate the identification of optimal values. Employing an optimization algorithm to analyze the dataset will create a predictive model for HRP. An optimal design guideline will be generated to develop the most cost-effective layout.

Chapter 2: Literature Review

2.1 Comparison of Research Work Across Different Studies

Over the years, various experimental setups were developed to examine how design parameters affect the pump's performance. This analysis facilitated the optimization of design parameters for the best performance. **Table 1** provides a summary of efficiency comparisons across different experimental setups.

Study	Drive Head, H_d (Inch)	Delivery Head, H_D (Inch)	Drive Pipe Diameter, D_d (Inch)	Efficiency, η (%)
Xingley Guo (2018)	78.74-106.29	Up to 1968	0.521	50-70
Young (1996)	108.66-127.96	Up to 5511.81	3.93	57.3
Wanchai (2019)	78.74-98.42	196.85-629.92	2.08	10-22
Kriaa (2025)	54.33-66.14	75.98	2.08	4.8 -10.4
Jafri (2020)	39.37	393.79	3	36.44-67.66

Table 1 : Result Comparison of Different Studies

2.2 Advancement in Waste Valve Geometry and Design

The waste valve constitutes a crucial component within a hydraulic ram pump. The design and configuration of the waste valve significantly influence the pump's performance. Water continually flows through the waste passage until reaching a threshold limit that triggers the closure of the valve. Numerous studies have been conducted on the development of waste valves since it is a crucial pump parameter. In the study of 5 | P a g e Surada et al. [8], it was found that increasing valve stroke will produce more impulse force, which helps to pump water more quickly. The experiment helped to find optimal stroke length and valve weight. Surada et al. [9] showed that orifice and disk diameter impact the water flow pattern significantly. Another study by Li et al. [10] used different thickness disk and offered a design that will decrease head loss by 45%. This waste valve design doesn’t have any spring attached, and sealing is made of soft material. Johanis et al. [11] tried different combinations of stroke length and weight to find the best combination that will work smoothly in a pump

2.3 Advancement in Pipe Configuration and Dimensions

Over the years, the dimensions of the drive and delivery pipes have been studied to improve operational efficiency. Pipe length and diameter, along with different assembly configurations, were studied by Young et al. [12], which designed a theoretical pump system equation with empirical factors that are dependent on ram pump size, delivery head, drive pipe thickness, and the waste valve configuration. Study by Najm et al. [13] performed a numerical model to simulate flow in all components. Their study derived equations that can predict performance and optimize pipe dimension, valve timing, and air chamber size. Sharma et al. [14] worked with different drive pipe setup configurations. Their study showed that adding a second drive pipe connecting with the same air chamber can increase efficiency by 14%. Guo et al. [15] developed two types of structure of pipe named front enlargement and back enlargement. They found that the back enlargement structure provides lower head loss and drag coefficient. Study by Mado et al. [16] constructed three configurations of different arrangements of components and found that the arrangement of inlet, waste valve, air chamber, and waste valve again gives the highest discharge in the delivery section when the waste valve was 367 gm

2.4 Advancement in Elevation Head in Drive and Delivery

The drive head refers to the height of the source water, which provides the force to ensure continuous flow. The delivery height is the elevation that the pumped water reaches. Major and minor head loss, drag, and friction coefficient are all related to elevation head. Asvapoositkul et al. [17] demonstrates that increasing drive head results in higher supply flow rate, delivery flow rate, and efficiency. Study done by Manohar et al. [18] found that the efficiency of the pump decreases with the change of delivery height in ascending order. But the efficiency increased significantly when the drive head was 2, 4, and 6 times the delivery head. Karim et al. [19] showed variation in drive head to delivery distance, and found that, high drive head gives a higher flow rate, but waste discharge rate also increases, for which the overall efficiency doesn’t improve.

2.5 Gaps in Current Knowledge

Though hydraulic ram pumps have performed well in rural water supply uses, several issues still exist, especially in maximizing their efficiency under changing flow circumstances. One of the main drawbacks of current studies is the dearth of thorough field studies evaluating hydraulic ram pumps across a broad spectrum of environmental and operating circumstances. Many research emphasizes controlled experimental settings that do not completely mimic the dynamic characteristics of real-world applications, like as water flow rates and seasonal variations in water supply. Furthermore, while the hydraulic ram pump has been effectively employed in rural regions, its employment is still limited by the availability of appropriate topographical conditions. Though many distant towns may not have such perfect circumstances, this technique is best suited for sites with significant elevation difference between the water source and the pump. Research is required on changes or inventions enabling the hydraulic ram pump to be employed in a more broad geographical range. The integration of hydraulic ram pumps with contemporary water management systems is another field yet under-researched. Though the technology is dependable and inexpensive, putting it into current water delivery system calls for meticulous design and planning. Studies investigating the viability of integrating hydraulic ram pumps with other water management technologies such as solar-powered systems to provide a more complete solution to off-grid water delivery are increasingly necessary.

2.5 Relevant Technologies and Methods

Primarily using the water hammer effect, hydraulic ram pumps operate; this effect results from the fast deceleration of water flow, which creates a pressure surge utilized to raise water to a greater height. This straightforward design lets the pump run without relying on outside power sources as electricity or fuel. Often, research on the hydraulic ram pump looks at the main parts impulse valve, check valve, and air chamber—to maximize performance [9]. These papers investigate how the design of every part influences the general efficiency and performance of the pump. Recent developments in materials science have helped build more affordable and durable hydraulic ram pumps. Using composite rubber for valve seals, for example, has improved the pump's lifetime by lowering wear and tear during cyclic operation. Research on computational fluid dynamics (CFD) has also assisted in optimizing the design of the water flow route via the pump. CFD models let engineers forecast how water will behave within the pump and find places where efficiency may be enhanced. When developing pumps for certain site circumstances, these tools are very useful as they help to guarantee the system is efficient and reasonably priced. The price of constructing and running the pump is a major concern in rural regions with poor infrastructure. Many research have suggested affordable materials and building methods to increase the accessibility of the hydraulic ram pump. Using PVC tubing for the pump's primary construction, for instance, greatly lowers the material cost without sacrificing performance. Hydraulic ram pumps have been appealing for communities in underdeveloped nations since the cost of building and upkeep has made them so. Water supply systems are usually underfunded.

Chapter 3: Description of the System

3.1 System Description and Specification

Hydraulic Ram Pump is a water lifting device that works on the principle of water hammer effect to elevate water from the reservoir without using any external power source. The driven water gets divided into two portions, waste portion and delivered portion. It operates solely on the energy of flowing water, making it sustainable and cost effective.

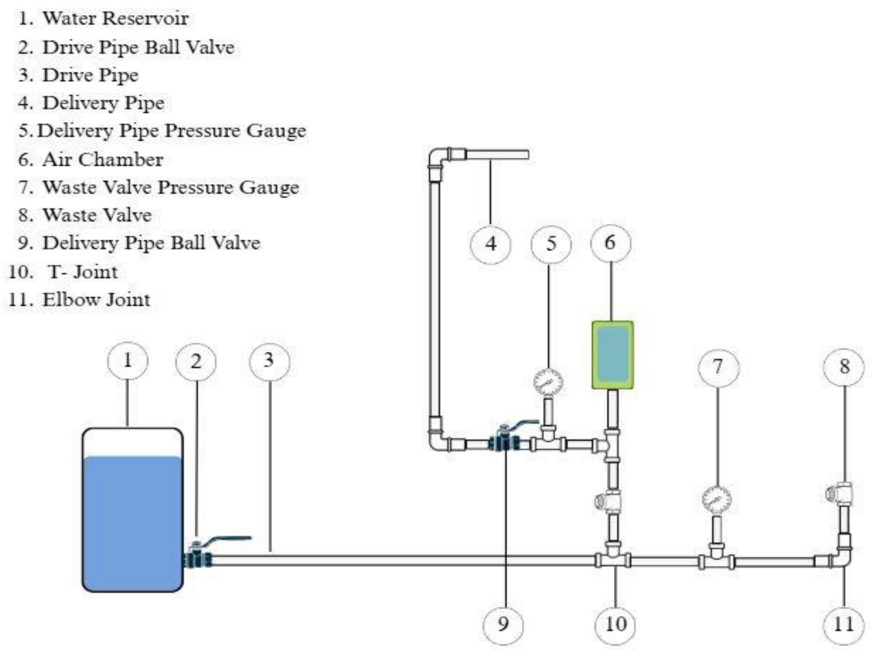

Figure 1: Schematic Diagram of Hydraulic Ram Pump Experimental Setup

3.1.1 Reservoir and Inlet Assembly

The experimental rig frame supported both the plumbing network and an elevation platform designed for the water reservoir. The feed reservoir itself was a 100 L nylon drum, selected for its lightweight structure and chemical inertness. A similar frame-based approach has been widely employed in prototype ram pump studies [22]. Prior experimental investigations have emphasized the sensitivity of ram pump performance to reservoir elevation, with drive head acting as the fundamental driver to delivery head and efficiency [23], [24], [25]. To allow systematic control, the reservoir stand incorporated a screw-jack mechanism capable of 0.25 m incremental adjustments, enabling tests across a supply head range of 10–40 inches consistent with methodologies employed in recent optimization studies [25], [26]. Water was drawn from the reservoir through a 25 mm tank nipple adapter and regulated by a manually operated stainless-steel ball valve (DN 25), which provided fine adjustment of the inflow rate. Downstream of the valve, the supply entered a 1- inch (≈ 25 mm ID) CPVC drive pipe of 78-242 inches in length. The drive pipe's geometry is a critical determinant of water hammer dynamics, as both length and diameter influence surge magnitude, timing, and cycle frequency. The chosen dimensions were calculated to achieve a surge period of ~0.12 s under 8 | P a g e nominal head conditions, aligning with experimental values reported in prior studies of hydraulic ram performance [23], [27], [28]. CPVC was employed for both the drive and delivery lines owing to its corrosion resistance, dimensional stability under cyclic loading, and proven cost-effectiveness in smallscale rural water applications [26], [27]. At the downstream end of the drive pipe, a 90° CPVC elbow fitting directs the flow into a custom-machined brass impulse (waste) valve. This valve, with a 12.5 mm orifice diameter, operates automatically: it is forced open by the incoming flow until a threshold velocity is reached, then snaps shut under backpressure, initiating the water hammer effect [23].

3.1.2 Impulse Valve and Pressure Surge Generation

The brass impulse valve, also referred to as the waste valve, operated as a self-actuating, spring-loaded mechanism. As water accelerated down the drive pipe, the valve momentarily remained closed until upstream pressure overcame the spring preload; it then snapped open, releasing a slug of water and creating a sudden pressure drop. When the valve slammed shut again under reduced flow, a high-pressure surge central to the ram pump action propagated upstream. This cyclical opening and closing generated the intermittent "water hammer" surges that drive a fraction of the inlet water into the delivery line.

3.1.3 Air Chamber and Surge Dampening

Conventional ram pumps use a rigid PVC or steel chamber as the catchment for rebound pressure, but several studies used a 20 L disposable polycarbonate bottle as the pressure chamber to test the influence of chamber elasticity and volume [22], [23]. Polycarbonate offers sufficient tensile strength to withstand great internal pressures. In this study, for air chamber, a 4-inch PVC pipe is used with two endcaps sealing it. The chamber's inlet is connected via a T-joint immediately downstream of the impulse valve, and its outlet feeds the delivery line through a brass check valve to prevent backflow. Prior to each test, the air chamber was pre-charged to 150 mbar (±5 mbar) using a calibrated hand pump in conjunction with a WIKAA 10 digital pressure gauge (accuracy ±0.5 %). The residual volume of air was determined by filling the chamber with water and measuring the displaced fraction, which consistently produced an air-to-water ratio of approximately 30 %. An appropriately sized chamber mitigates destructive pressure spikes while stabilizing the delivery head, thereby improving overall pumping efficiency [29].

3.1.4 Delivery line and Discharge Control

From the air chamber, pressurized water entered a second CPVC pipe (also 25 mm nominal diameter) that conveyed the flow to an elevated discharge point set 48-152 inches above the pump assembly. A ball valve near the chamber outlet served as a throttle, enabling adjustment of backpressure and fine-tuning of flow rate versus delivery head. Downstream of this valve, a second pressure gauge monitored the stabilized delivery pressure. Excess water not directed into the delivery line was expelled through the impulse valve waste port, completing the cycle and initiating the next surge.

3.1 Working Procedure of Hydraulic Ram Pump

A hydraulic ram pump (hydram) is a water pump that operates without external power sources such as fuel or electricity. It functions on the principle of the water hammer effect. The main parts include the drive pipe, waste valve, air chamber, and delivery pipe. The total cycle time can be divided into 4 distinct periods as it is mentioned by Schiller et al. [30]. In Period A, depicted in **Fig. 2(a)** the water flows steadily through the drive pipe from a source, building high momentum under the effect of the drive head, Hd. When the flow velocity is below the waste valve's threshold, water passes easily through it. At the threshold velocity the total drag and pressure forces on the waste valve is equal to its weight, and thereafter the valve begins to close. In Period B, presented by **Fig. 2(b)**, from the start to closing, the waste valve comes to a complete shut-off. The water that escapes during this period does not have any impact on the cycle performance. So, it is considered a loss, and good design of waste valve ensures a quick shut-off to prevent this water loss. In Period C of **Fig. 2(c),** after the sudden closure of waste valve, according to the water hammer effect, stopping a high-momentum flow causes a pressure surge. This surge pushes water into the air chamber, which initially contains air; as water enters, it compresses the air. This compression transforms kinetic energy into pressure energy, forces the delivery check valve to open, and pushes water through the delivery pipe, creating elevation head. For Period D, scheduled in **Fig. 2(d),** the air chamber empties and pressure drops, hence, the delivery valve closes. The pressure next to the check valve significantly exceeds the static supply pressure, resulting in a reversal of flow towards the supply source. This motion is referred to as recoil. Once the drive flow velocity becomes higher than the waste valve's threshold, the waste valve opens again, repeating the cycle. The aforementioned description of the process is predicated on averaged effects. The fast operation of the waste and delivery valves generates pressure pulsations that overlay the primary effects of consistent pressure differentials and fluid column inertia. These pressure fluctuations generate compression waves that overlay the velocity variations. Taking all of these factors into account would result in a very intricate study.

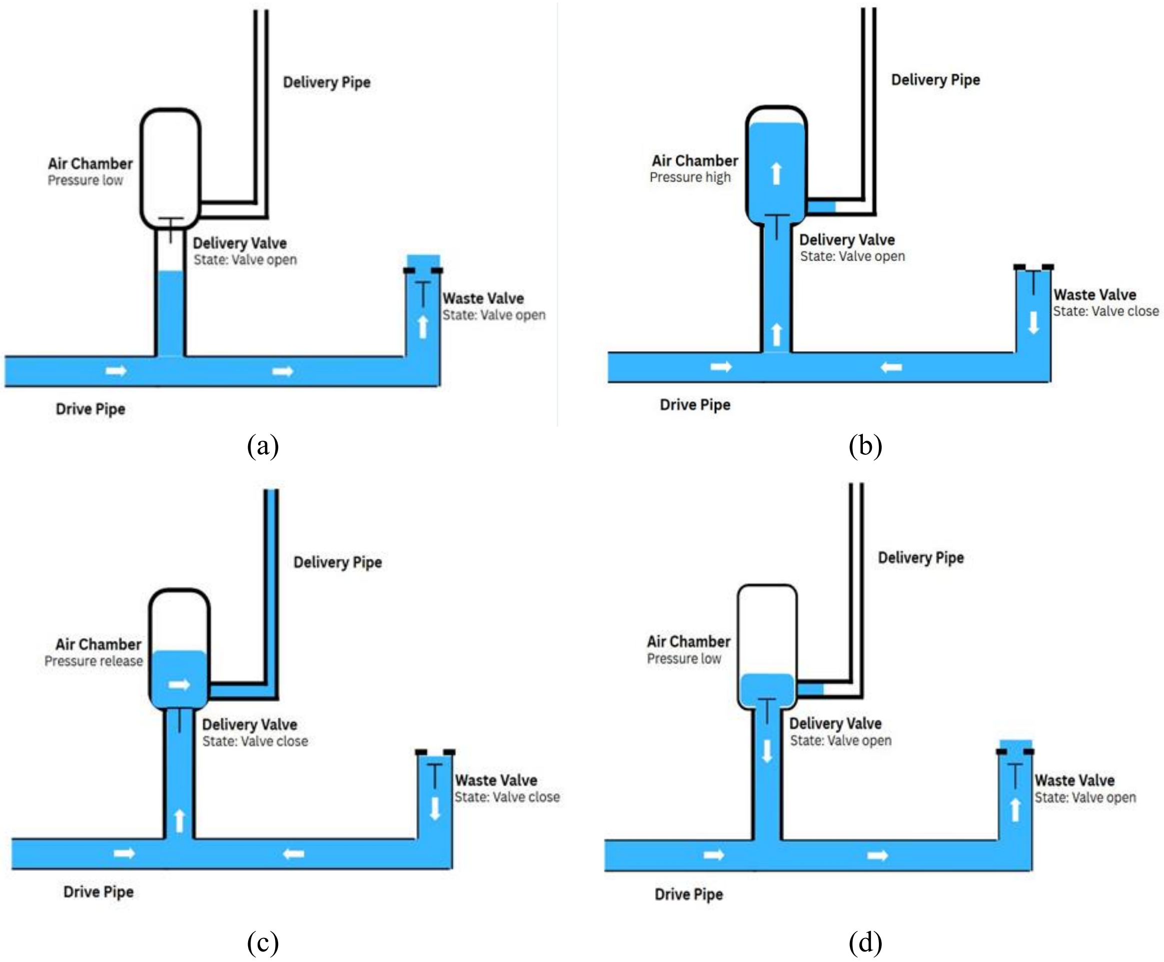

Figure 2: Working Procedure of HRP

3.2 Operating Conditions

The hydraulic ram pump's performance is highly sensitive to various operating conditions. In order to study the impact of different parameters like drive pipe length (L), drive head (H_d), delivery head (H_D), air chamber volume (V_A), and pipe diameters on the performance, cost and critical delivery head (H_C) of the pump, different design cases are analyzed. The experimental investigation was conducted under a comprehensive range to assess the performance of the hydraulic ram pump in detail. The conditions proposed by R. Fatahi-Alkouhi et al. [24] are used in the experimental study. H_d and H_D range was changed to accommodate locally available material. Within the range mentioned in **Table 2**, several instances are examined to study the effect of various input parameters on the output parameter.

Variable	Unit	Range of changes
Drive head, $\boldsymbol{H_d}$	inch	13.00 – 25.00
Delivery head, $\boldsymbol{H_D}$	inch	48.00 - 152.00
Drive pipe length, *L*	inch	78.00 – 242.00
Drive pipe diameter, $\boldsymbol{D_d}$	inch	0.75 – 1.25
Delivery pipe diameter, $\boldsymbol{D_D}$	inch	0.50 – 1.25
Air chamber volume, $\boldsymbol{V_A}$	L	1.03 – 5.35
Weight of impulse valve (flange), $\boldsymbol{W}$	N	0.3924
Average area of waste valve (flange), $\boldsymbol{A_d}$	mm^2	490.88
Length stroke of impulse valve, *s*	mm	2.00
Loss factor, *HVD*	-	59
Loss factor, *RS*	-	85
Loss factor, *N*	-	76
Friction factor, *f*	-	0.007 [32]
Drag coefficient, $\boldsymbol{C_d}$	-	0.6 [33]
Specific weight of water, $\boldsymbol{\gamma}$	N/m^3	9810
Bulk modulus of water, *K*	Pa	2.2×10^9
Modulus of elasticity of PVC pipe, *E*	GPa	3.00 [32]
Thickness of pipe, $\boldsymbol{t_d}$	mm	3.00

Table 2 : Condition of Parameters Used in the Study

3.2.1 Variation in drive pipe length

As highlighted by Kesharwani et al. [25] drive pipe length (L) is a critical parameter to consider in the design of a hydraulic ram pump. According to Inthachot et al. [26] drive pipe length depends on the drive head of the pump. So, apart from the L, drive head-drive pipe length ratio (*h/L*) is also identified as a design parameter. **Table 3** presents the drive pipe lengths ranging from 78 inches to 242 inches across a total of 10 cases. This analysis aims to determine how the efficiency and critical drive head vary with different drive pipe lengths. Other design parameters like H_D, H_d, D_d, D_D are kept constant. For all 10 cases H_d is fixed at 25 inch, therefore *h/L* ratio traverses between 3.12 to 9.68 units

Design Case	Drive Head, H_d (inch)	Drive Pipe length, L (inch)	Drive head-Drive pipe length Ratio, h/L	Drive Pipe Diameter, D_d (inch)	Delivery Pipe Diameter, D_D (inch)	Delivery Head, H_D (inch)
1	25	78	0.321	1	1	65
2	25	104.5	0.239	1	1	65
3	25	120	0.208	1	1	65
4	25	145	0.172	1	1	65
5	25	170	0.147	1	1	65
6	25	184	0.136	1	1	65
7	25	195	0.128	1	1	65
8	25	210	0.119	1	1	65
9	25	228	0.110	1	1	65
10	25	242	0.103	1	1	65

Table 3 : Study of Effect on HRP for variations of Drive Length

3.2.2 Variation of delivery head

The study of Guo et al. [27] demonstrates that altering the delivery head significantly impacts both efficiency and the flow rate within the delivery pipe. In **Table 4** H_D varies from 48 to 152 inch. The limited space of the laboratory restricted the utilization of a wide range of delivery heads. Further, in Asvapoostkul et al. [28] another parameter drive head-delivery head ratio (*h/H*) is mentioned, which provides us with a direct relation between the two heads and their impact on each other. In all 10 cases, H_d is maintained at 25 inches, resulting in an *h/H* ratio that ranges from 0.521 to 0.1645 units.

Design Case	Drive Head, H_d (inch)	Drive Pipe length, L (inch)	Drive Head-Delivery Head Ratio, *h/H*	Drive Pipe Diameter. D_d (inch)	Delivery Pipe Diameter, D_D (inch)	Delivery Head, H_D (inch)
1	25	120	0.521	1	1	48
2	25	120	0.49	1	1	51
3	25	120	0.385	1	1	65
4	25	120	0.291	1	1	86
5	25	120	0.263	1	1	95
6	25	120	0.225	1	1	111
7	25	120	0.203	1	1	123

8	25	120	0.184	1	1	136
9	25	120	0.1724	1	1	145
10	25	120	0.1645	1	1	152

Table 4: Study of Effect on HRP for variation of Delivery Head

3.2.3 Variation of air chamber volume

The performance of the pump is directly affected by variations in the volume of the air chamber. The studies [29] [30] illustrates the effect of air chamber volume (V_A) on efficiency. In **Table 5** a total of seven distinct volumes of air chambers are tabulated, utilizing a 4-inch diameter PVC pipe. The height of the pipes is different, hence the different volume is achieved. Cylindrical end parts of the pipe are sealed with two N-POLY endcaps, making it air-tight. Other parameters were kept constant as shown in **Table 4**.

Design Case	Drive Head, H_d (inch)	Drive Pipe length, L (inch)	Air Chamber Volume, V_A (L)	Drive Pipe Diameter, D_d (inch)	Delivery Pipe Diameter, D_D (inch)	Delivery Head, H_D (inch)
1	25	120	1.03	1	1	65
2	25	120	1.61	1	1	65
3	25	120	2.06	1	1	65
4	25	120	3.09	1	1	65
5	25	120	3.71	1	1	65
6	25	120	4.53	1	1	65
7	25	120	5.35	1	1	65

Table 5: Study of Effect on HRP for variation of Air Chamber Volume

3.2.4 Variation of drive pipe length-drive pipe diameter ratio

In **Table 3**, only drive pipe length was varied, whereas according to R. Fatahi-Alkouhi et al. [31] changing drive pipe diameter along with the drive pipe length can provide more dynamic design parameters. Table 5 denotes both L and D_d varying simultaneously, and hence the main design parameter here is the drive pipe length-drive pipe diameter ratio (*L/D*), which is taken periodically. Twelve design cases were evaluated with *L/D* ratios varying from 104 to 322.67, achieved through different combinations of pipe lengths (78-242 inches) and diameters (0.75-1.25 inches). The heads H_d and H_D are kept constant at 25 inches and 65 inches, respectively.

Design Case	**Drive Head, H_d (inch)**	**Drive Pipe length, *L* (inch)**	**Drive Pipe Diameter, D_d (inch)**	**Delivery Pipe Diameter, D_D (inch)**	**Drive Pipe length-Drive Pipe Diameter Ratio *L/D***	**Delivery Head, H_D (inch)**
1	25	78	0.75	0.50	104	65
2	25	145	0.75	0.50	193.33	65
3	25	195	0.75	0.50	260	65
4	25	242	0.75	0.50	322.67	65
5	25	78	1	0.50	78	65
6	25	145	1	0.50	145	65
7	25	195	1	0.50	195	65
8	25	242	1	0.50	242	65
9	25	78	1.25	0.50	62.4	65
10	25	145	1.25	0.50	116	65
11	25	195	1.25	0.50	156	65
12	25	242	1.25	0.50	193.6	65

Table 6: Study of Effect on HRP for variation of Drive Pipe Length- Drive Pipe Diameter Ratio

3.3 Data Acquisition

Various measuring tools and equipment implied in **Table 7** were employed to assess the operational data accurately. A flow meter (0- 100 L/min) was utilized to record the waste flow rate and delivery flow rate. External influences, such as pipe friction, air, and other factors, may cause slight deviations in the results. Two distinct pressure gauges were positioned at different locations: a 0-500 mbar pressure gauge was installed on the drive pipe, as this section experiences relatively higher water pressure compared to the delivery and waste pipe sections. For the delivery pipe, a pressure gauge with a measuring range of 0-300 mbar and an accuracy tolerance of 0.25% was used. To record the time required for flow rate calculations in the waste valve and delivery pipe, a stopwatch was employed; the timing was conducted manually, which may introduce minimal variations. To measure the volume of water delivered by the pump and the amount flowing through the waste valve, a 500 mL plastic beaker and a 5-gallon cylindrical bucket were used. The beaker was held manually to collect pumped water; due to the height disparity, approximately 0.01 mL of water splashed from the bucket. For measuring pipe dimensions, a 100-foot measuring tape was utilized. Additionally, a 0- 5 L measuring cylinder was used to determine the volume of the air chamber measured.

Device/tool	Measured parameter	Measuring range	Measuring accuracy
Flow meter	Flow rate of delivered water and wastewater	0–100 L/min	±1% of reading
Pressure gauge	Ram pump outlet pressure	0–500 mbar	±0.25%
Pressure transducer	Continuous measurement of delivery and waste line pressures	0–0.9 MPa	±0.1% FS
Stopwatch	Period of valve beat counts and flow calibration timing	–	±0.01 s
Plastic beaker	Quantity of water delivered (small-scale calibration)	500 mL	±0.01 mL
Cylindrical bucket	Quantity of wastewater (bulk measurement)	5 gal	–
Caliper	Depressed water level at discharge inflow and wastewater	0–150 mm	±0.01 mm
Long tape measure	Critical delivery head height	0–100 ft	±0.001%
Measuring cylinder	Air chamber internal volume	0–5 L	±0.5%
Surveyor's level	Drive head height measurement	0–50 ft	±0.05%

Table 7: Measuring Tools and Devices Used in Ram Pump Experimental Setup

3.4 Criteria for Component Selection

Several critical factors were used to pick components for the hydraulic ram pump, with the goal of assuring efficiency, cost-effectiveness, durability, and simplicity of maintenance. The following variables were examined throughout the selecting process:

• **Functionality:** Each component was chosen for its capacity to execute the various duties necessary for the hydraulic ram pump's optimal functioning. For example, the impulse valve was chosen due to its capacity to create the required pressure surge via water hammer.

• **Durability:** The components' materials were selected based on their capacity to survive mechanical loads and climatic conditions seen in off-grid, rural settings. Durability was especially critical for moving elements like the impulse valve, check valve, and rubber seals, which are subjected to constant wear during operation .

• **Cost:** The total cost of the hydraulic ram pump system was an important consideration while choosing components. The design intended to save costs by using locally accessible materials, reducing the need for costly imports while yet achieving functional and durability criteria.

• **Availability**: The components were chosen according to the availability of materials in local markets. This allows for easy repairs and replacements in distant places where access to specialist components may be restricted.

• **Maintenance:** The hydraulic ram pump's design stressed simplicity of maintenance in order to save downtime and labor expenses. Components that need regular maintenance were eliminated, and the system was developed with simplicity in mind, resulting in fewer moving components and possible failure areas

3.5 Material Used

The materials selected for the construction of the hydraulic ram pump were chosen to optimize the balance between cost, performance, and durability. The main materials used for the various components are outlined below:

Component	Material	Explanation
Drive Pipe	**PVC (Polyvinyl Chloride)**	PVC was selected for the drive pipe due to its low cost, ease of installation, and resistance to corrosion. It is lightweight, durable, and easily available in local markets, making it ideal for rural water systems. PVC also has good pressure resistance, which is crucial for the hydraulic ram pump's operation.
Delivery Pipe	**PVC (Polyvinyl Chloride)**	Like the drive pipe, the delivery pipe was made from PVC for the same reasons: cost-effectiveness, durability, and ease of assembly. It also offers excellent resistance to chemicals, making it suitable for long-term use in water systems.
Impulse Valve	**Brass**	The impulse valve, also known as the waste valve, was made of brass due to its high strength and resistance to corrosion, which ensures durability under the high pressure created during the water hammer effect. Brass also resists wear and tear, which is important for the cyclical operation of the valve.
Check Valve	**Brass**	The check valve was made of brass for similar reasons as the impulse valve. Brass is durable, resistant to corrosion, and performs well under pressure. The check

Component	Material	Explanation
		valve prevents backflow, ensuring the system functions efficiently.
Rubber Gaskets	**Rubber**	Rubber gaskets were chosen to create airtight seals within the valve components. Rubber is flexible, resilient, and forms tight seals even under pressure, which is essential for preventing leaks and maintaining consistent performance.
Air Chamber	**Steel Reinforced PVC**	The air chamber was constructed from steel or reinforced PVC, depending on availability. The air chamber plays a crucial role in smoothing out pressure fluctuations within the pump system. Steel was chosen for its high strength and durability, whereas reinforced PVC provides a lightweight alternative that also resists corrosion.
Valve Stems & Critical Components	**Stainless Steel**	Stainless steel was used for the valve stems and other critical components exposed to mechanical stresses and wear. Stainless steel is highly resistant to corrosion, ensuring that these components maintain their integrity over time. It also offers high tensile strength, which is necessary to withstand the forces applied during the pump's operation.
Water Tank	**Polyethylene or Steel**	The water tank, which stores the pumped water, was typically constructed from either high-density polyethylene (HDPE) or steel, depending on the availability and cost . HDPE is lightweight, resistant to corrosion, and highly durable, making it a suitable option for long-term water storage. Steel tanks, on the other hand, offer greater structural strength but are heavier and more expensive.
Flow Sensors & Pressure Gauges	**Plastic and Metal**	The flow sensors and pressure gauges, used to monitor the pump's performance, were made from durable

Component	Material	Explanation
		plastics and metals like stainless steel. These materials ensure that the sensors and gauges can withstand the pressures and environmental conditions in the field. Stainless steel parts are resistant to rust and corrosion, which is essential for components exposed to water and outdoor conditions.

Table 8: Overview of the materials selected for each component of the hydraulic ram pump

Chapter 4: Computational Methodology

4.1 Governing Equations

The main goal of this experiment is to find out the efficiency and critical drive head with delivery flow rate trade-offs. The analytical model developed by Schiller et al. [30] predicts the performance of HRP most accurately, hence it is used to find out the theoretical efficiency and delivery flow rate in this study.

For Period A, the usual one-dimensional unsteady flow approximation and steady flow equations can be defined between (1) and (8) of **Fig. 1**, when the water in the drive pipe accelerates with a constant drive pipe diameter, length, and friction factor can be defined as follows,

$$\frac{L}{g}\frac{dv}{dt} = H_d - (1 - \sum h_L + f\frac{L}{D} + RS)\frac{V^2}{2g} \qquad (1)$$

Where, H_d is the static drive head of the HRP, $\sum h_L$, is the total minor losses in the system, including bends and other components. f is the friction factor of the drive pipe, and RS is the total head loss factor of the waste valve when fully open, V is the velocity of water in the drive pipe, L is the drive pipe length, and g is the acceleration due to gravity. The total head loss (including minor and major) can be defined as M, a constant, as follows,

$$M = 1 + \sum h_L + f\frac{L}{D} + RS \qquad (2)$$

In period A, an acceleration continues till a threshold velocity V_0 is attained when the total drag force on the waste valve equals its weight, W. A_v is the project surface area, γ defines the specific weight of water and C_d is the drag coefficient of the waste valve. V_0 can be defined as,

$$V_0 = \sqrt{\frac{2gW}{C_d A_v \gamma}} \qquad (3)$$

At $\frac{dv}{dt} = 0$, the average steady flow velocity in the cycle period A, V_s is calculated by the following equation,

$$V_s = \sqrt{\frac{2gH_d}{M}} \qquad (4)$$

The ratio of threshold flow velocity and average steady flow velocity is defined as,

$$m = V_0/V_s \tag{5}$$

For the pump to operate perfectly, the value of m must be between 0 to1. The volume of total supplied water during period A, V_{sp1} is obtained by,

$$V_{sp1} = \frac{LA}{M} \times \left[\ln\left(\frac{1.0}{1.0 - \left({V_0}^2 / {V_s}^2 \right)} \right) \right] \tag{6}$$

When $V_0 = V_s$, $(m = 1)$ the amount of total water supplied, V_{sp1} will be infinite, implying that the pump will not supply any water to create an appropriate pressure head. The time duration during period A is $t_1$which is obtained by integrating equation (1) where H is the supply head.

$$t_1 = \left(\frac{L^2}{2gH_dM} \right)^{1/2} \times \ln\left[\frac{1.0 + m}{1.0 - m} \right] \tag{7}$$

It is evident from above that the waste valve remains open until the constant flow velocity Vs is reached in the drive pipe, so that when $V_0 = V_s$ cycle time $t = \infty$ and the valve will not shut at all. In that scenario, m will equal 1, and the maximum allowable weight of the waste valve is determined at the specified driving head. This specific scenario is defined as the critical drive head. The time duration during period B is t_2 when the waste valve closes instantaneously, can be denoted by,

$$t_2 = \leq \frac{2L}{c} \tag{8}$$

Here c is the wave celerity, which denotes the wave speed of the flowing water and can be written as,

$$c = \sqrt{\frac{K_c}{\rho}} \tag{9}$$

Where K_c is the composite modulus of elasticity of water and pipe, and ρ is the density of water. Further K_c is obtained by the equation,

$$K_c = \frac{1.0}{\left(\frac{1}{K} + \frac{D_D}{Et_p} \right)} \tag{10}$$

Where K is the bulk modulus of water, E is the modulus of elasticity of the pipe material and t_p is the pipe thickness. In period C, when the delivery valve is opened and HRP starts to pump water, there is a major head loss due to friction. The total head loss in the delivery region can be characterized by the following,

$$h_r = HVD\frac{V_0{}^2}{2g}\left(1 - \frac{H_D}{h_{max}}\right) \tag{11}$$

Where H_D is the average static delivery head and h_{max} is the maximum delivery head that can be theoretically obtained with a smooth pipe without any friction losses. In this equation HVD is the friction loss coefficient of the delivery valve, which is obtained iteratively in experimental process. The maximum flow velocity through the drive pipe during period C, V_3 is obtained by,

$$V_3 = V_0 - (H_D + h_r)\left({}^{g}/_{c}\right) \tag{12}$$

The theoretical maximum delivery head without any losses of HRP is denoted by,

$$h_{max} = \frac{c}{g}V_0 \tag{13}$$

Further, the time duration during period C is t_3, which is the total time starting from water flowing into the air chamber until the delivery valve completely shuts off. This cycle time is formulated as,

$$t_3 = \left(\frac{2L^2}{gH_DN}\right)^{1/2} \times \tan^{-1}\left\{\left(\frac{NV_3{}^2}{2gH_D}\right)^{1/2}\right\} \tag{14}$$

Where N is the head loss factor concerning the drive pipe and delivery valve. The quantity of water supplied to the delivery in this period can be defined as,

$$V_{sp3} = \frac{LA}{N} \times \left[\ln\left(\frac{NV_3{}^2}{2g} + 1.0\right)\right] \tag{15}$$

V_{sp3} is the useful water that is delivered by the ram pump. The duration of period D is estimated as the time needed for a pressure wave to fully reflect and complete on cycle. After this, the remaining pressure waves in the drive pipe are considered insignificant compared to the main flow and steady pressure differences,

$$t_4 = \frac{2L}{c} \tag{16}$$

So, the total cycle time for one complete pump to delivery of the HRP system can be defined as the summation of all four periods,

$$T = t_1 + t_2 + t_3 + t_4 \tag{17}$$

This is the average time period for a single cycle to be completed of HRP system. The supply and delivery flowrate can be found by dividing the volume of water supplied and pumped to the average time,

$$Q_S = V_{sp1}/T \tag{18}$$

$$Q_d = V_{sp3}/T \tag{19}$$

The efficiency of the HRP is calculated by the D'Abbusion equation,

$$\eta = \frac{H_D \times Q_d}{H_d \times Q_S} \tag{20}$$

4.2 Multi-objective optimization

The goal of multi-objective optimization is to maximize η and Qd, while reducing the HC and Ct. The input parameters and their respective ranges used for the inquiry are shown in **Table 1**. Initially, all experimental data from **Tables 8,9,10,11** were congregated into a single data file which was then fed to a hybrid machine learning model. The compiled file consists of 39 sets of experimental data. As the number of training datasets is lower here, certain challenges arise, primarily related to overfitting and generalization. To eliminate this problem a regression analysis was conducted to generate a quadratic function of the output parameters. Using RSM, 5000 synthetic samples were generated within the range described in **Table 1**. This augmented dataset was then integrated with a hybrid model combining Artificial Neural Networks (ANN) and XGBoost for optimization. The ensemble algorithm solver yielded 10 optimal design points, ranked hierarchically from 1 to 10. The chronology of the optimization methodology has been exemplified by the flowchart in **Fig. 11**

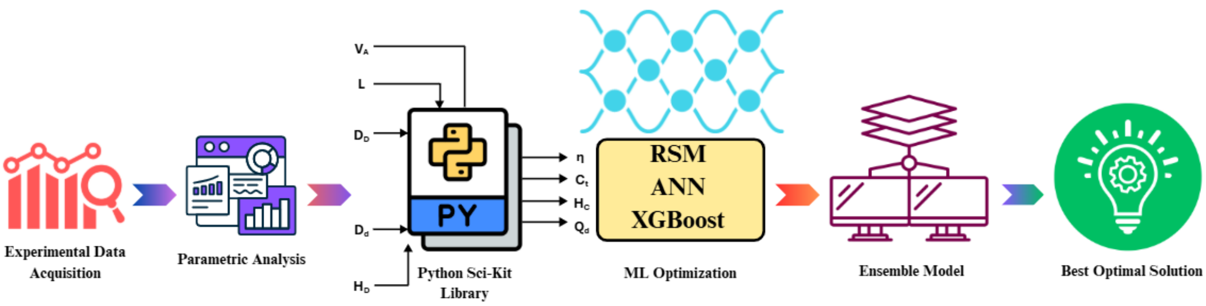

Figure 3: Flowchart of the optimization methodology

4.3 Model Validation

Validation of the developed hydraulic ram pump (HRP) model was performed by comparing the numerical predictions with experimental measurements obtained from the benchtop setup. The theoretical results had been validated against the works of Schiller et al. [30]. The primary performance indicators considered were the delivery flow rate (Qd) and the efficiency (η), since they directly reflect the hydraulic energy transfer within the system. **Table 8** presents the comparative results between experimental and model-predicted values across a range of delivery heads

Delivery Pipe Head, H_D (inch)	Theoretical Efficiency (%)	Experimental Efficiency (%)	Relative Error in η (%)	Theoretical Delivery Pipe Flow rate, Q_d (L/min)	Experimental Delivery Pipe Flow rate, Q_d (L/min)	Relative Error in Q_d (%)
48	59.04	58.12	1.56	2.136	2.105	1.45
51	57.92	56.668	2.16	1.97	1.912	2.94
65	53.09	50.06	5.71	1.3619	1.298	4.69
86	49.162	48.05	2.26	0.9286	0.874	5.88
95	43.53	40.64	6.64	0.712	0.668	6.16
111	36.82	34.794	5.50	0.501	0.46	8.19
123	31.51	29.13	7.55	0.379	0.343	9.54
136	26.39	24.42	7.46	0.258	0.231	10.29
145	23.35	20.4	9.12	0.203	0.178	12.14
152	18.29	14.33	11.05	0.1337	0.116	13.23

Table 9: Analytical analysis for different delivery heads

Table 8 presents the comparative results between experimental and model predicted values across a range of delivery heads of 48-152 inches. For efficiency measurements, the relative error ranged from 1.56% to 11.05%, with an average deviation of 5.40%. The lower delivery heads (48-65 inches) showed superior agreement with relative errors below 6%, while higher delivery heads (>136 inches) exhibited slightly larger deviations due to increased complexity in pressure dynamics and potential minor head losses not fully captured in the theoretical framework. The delivery flow rate validation showed comparable accuracy, with relative errors ranging from 1.45% to 13.23%. The flow rate predictions demonstrated systematic behavior where errors increased proportionally with delivery head, consistent with the compounding effects of friction losses and pressure drop uncertainties at higher elevations. **Fig. 4** provides a graphical comparison of efficiency and flow rate trends. The close overlap of curves indicates that the developed model successfully captures the governing physics of the water hammer and energy conversion phenomena. **Fig. 4** also captures similar trends that are shown by Schiller et al. [30]. Due to a lack of experimental data at the operating condition used in the Schiller et al. study, the exact parametric validation was not possible, but a strong match with the trend confirms the accuracy of the predicted model.

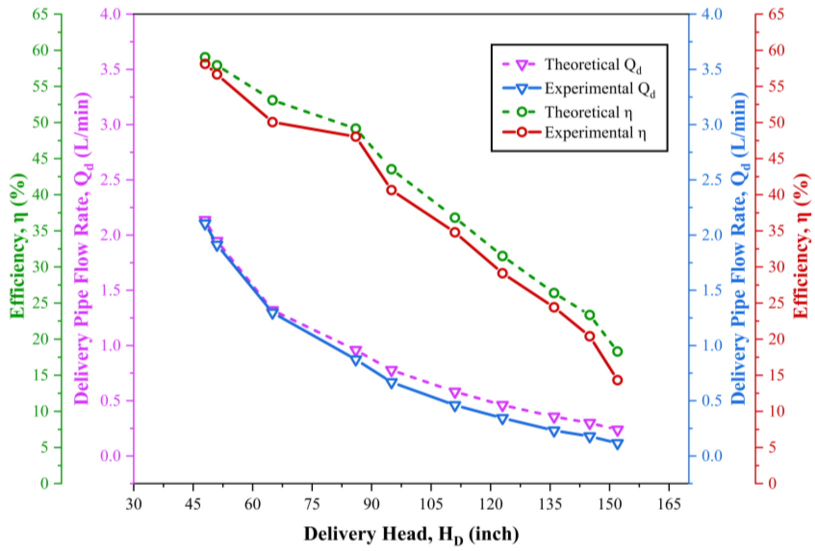

(a)

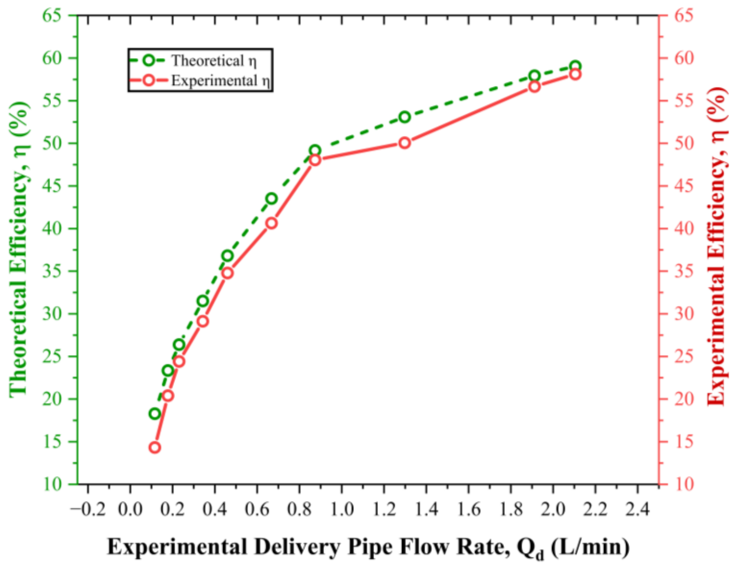

(b)

Figure 4: Validation of experimental HRP system against the work of Schiller et al. [30]

This validation confirms that the developed mathematical model provides reliable predictions for hydraulic ram pump performance within the tested parameter range, with maximum errors well below the 15% threshold typically considered acceptable for hydraulic system modeling. Therefore, the validated model forms the foundation for the subsequent optimization studies and provides confidence in the design guidelines derived from the theoretical analysis.

Chapter 5: Results and Discussions

5.1 Analysis of the Study

The purpose of this study is to develop a HRP system, to obtain high net efficiency and delivery pipe flowrate. Additionally, the study aims to reduce the total cost of the system (Ct), and critical drive head (HC) as much as possible. Moreover, comparison among the four key performance parameters has been studied.

5.1.1 Parametric Analysis

The design parameters selected for analysis and optimization are: Drive pipe length (L), Drive head (Hd), Delivery head (HD), Drive pipe diameter (Dd), Delivery pipe diameter (DD) and Air chamber volume (VA). Since, Hd and HD denotes the main heads that determine total energy conversion, so their impact on the performance is most significant. Similarly, DD and Dd controls the flow of the pump, L limits backlash, and VA smoothens the outlet flow. Therefore, these six key design parameters have been analyzed for the HRP system.

5.1.2 Effect of drive pipe length

Table 9 depicts the experimental results yielding the operating conditions proposed in **Table 3**. It shows that HRP provides the maximum η, which is 60.29 when L was 210 inches and minimum η, which is 42.8 when L was 78 inches. For H_C, highest value was found when L was measured as 242 inches and lowest was recorded at 78 inches. Similarly, maximum C_t was calculated at 242 inches and minimum at 78 inches. For, Q_d highest flow rate was recorded at 210 inches and the lowest at 78 inches.

Table 10: Experimental results of ram pump for variation of Drive pipe length

Design Case	Drive Pipe Length, L (inch)	Critical Drive Head. H_C (inch)	Air chamber pressure, V_A (mbar)	No of beats per min (N)	Drive Pipe Flow rate, Q_s (L/min)	Waste Valve Flow rate, Q_w (L/min)	Delivery Pipe Flow rate. Q_d (L/min)	Efficiency, η (%)	Total Cost, C_t ($)
1	78	13.4	190	76	6.324	5.283	1.041	42.80	267.85
2	104.5	13.7	182	57	6.746	5.482	1.264	48.72	289.95
3	120	14.1	178	50	6.742	5.444	1.298	50.06	302.85
4	145	14.3	171	42	6.659	5.299	1.360	53.10	323.65

5	170	14.5	168	36	6.623	5.211	1.412	55.43	344.55
6	184	14.8	166	33	6.633	5.163	1.470	57.62	356.15
7	195	15.0	165	31	6.670	5.170	1.50	58.51	365.35
8	210	15.1	165	29	6.727	5.167	1.56	60.29	377.85
9	228	15.25	164	26	6.660	5.191	1.469	57.35	392.85
10	242	15.4	162	25	6.580	5.224	1.356	53.59	404.55

From **Fig. 5(a)** it is evident, η showed a non-monotonic relationship with L, initially increasing from 42.8% at 78 inches to a maximum of 60.29% at 210 inches, before declining to 53.59% at 242 inches. This is because, lower drive pipe length tends to provide backflow of water to the supply region as it has less pressure difference. But after the critical point, efficiency tends to drop because the increasing friction in the feed pipe becomes dominant. H_C exhibited a steady increase from 13.4 inches to 15.4 inches as drive pipe length increased from 78 to 242 inches. This trend aligns with theoretical expectations, as longer drive pipes require higher minimum supply heads to maintain adequate pressure for valve closure and pumping operation. **Fig. 5(a)** also indicates that C_t increased linearly from \$267.85 to \$404.55 as drive pipe length increased from 78 to 242 inches, representing a 51% cost increase. This linear relationship primarily reflects the material cost of additional piping. The cost analysis reveals that the optimal efficiency point (210 inches) corresponds to a system cost of \$377.85, indicating a trade-off between performance and economic feasibility. On the other hand, while Q_s remained relatively stable (6.324-6.727 L/min), the Q_d increased from 1.041 to 1.56 L/min up to 210 inches before declining. This improvement in useful flow delivery contributed to the efficiency gains observed in the intermediate length range. Then **Fig. 5(b)** explains that efficiency peaks at 60.3% and optimal performance occurs when H_C is 15.1 inches. At higher critical heads, efficiency decreases by 11.1% after increasing by 40.9% from the minimum (42.8% at H_C = 13.4 inches) to the maximum. Throughout the H_C range, total cost rises 51% linearly, while delivery flow rate peaks at 1.56 L/min under ideal circumstances and synchronizes with efficiency trends. The ideal H_C is the point in the drive pipe system where friction losses are minimized and water hammer effects are maximized.

In **Fig. 5(c)** the correlation heat-map reveals strong interdependencies between design parameters and performance metrics. Drive pipe length (L) shows strong positive correlation with total cost (r = 0.89) and moderate correlation with critical drive head (r = 0.67), indicating that longer pipes require 67% higher minimum supply heads and increase costs by 89%. The drive head-drive pipe length ratio (h/L) exhibits strong negative correlation with efficiency (r = -0.52), demonstrating that lower h/L ratios (ranging from 0.321 to 0.103) improve performance by 52%. Efficiency shows moderate positive correlation with L (r = 0.52) and delivery flow rate (r = 0.48), confirming the non-monotonic performance relationship. The critical finding reveals strong negative correlation between efficiency and cost (r = -0.78), representing a 78% inverse relationship that highlights the fundamental performance-economics trade-off in hydraulic ram pump design.

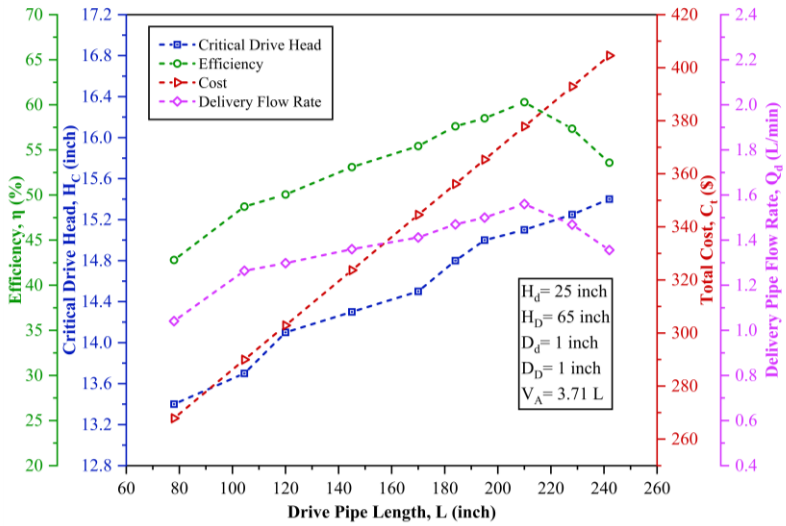

(a)

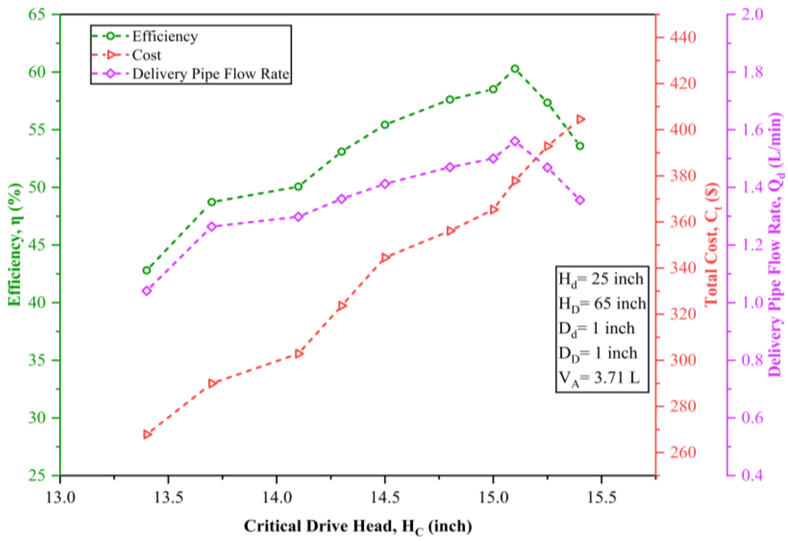

(b)

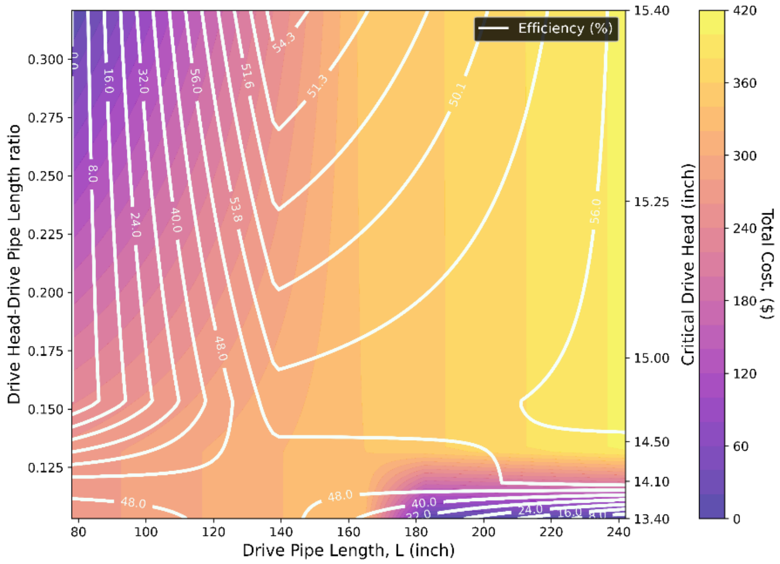

(c)

Figure 5: Effect of drive pipe length and delivery head on efficiency and total cost.

A positive correlation between V_A and *N* corresponding to *L* is given in **Fig. 6(a)** and **Fig. 6(b).** The number of beats per minute decreased substantially from 76 to 25 beats/min as length increased, indicating that longer pipes produce slower but more powerful strokes. The reduction in beat frequency with longer pipes suggests that while individual strokes become more powerful, the overall pumping rate decreases, ultimately reducing efficiency. Correspondingly, air chamber pressure decreased from 190 to 162 mbar, suggesting reduced pressure surge intensity but improved pressure stability with longer drive pipes. In **Fig. 6(c)** chart reveals the cost composition of the HRP system across drive pipe lengths from 78 to 242 inches. Pipe cost dominates the system economics, increasing from 50.5% ($135.2) at 78 inches to 65.9% ($266.8) at 242 inches, representing a 97.3% cost escalation. Fixed components show minimal variation: air chamber cost remains constant at $45-50 (16.8% to 12.4%), valve cost at $25-30 (9.3% to 7.4%), and sensor cost at $15-18 (5.6% to 4.4%). Accessories cost increases significantly from $18 to $35 (94.4% increase) due to additional fittings and supports required for longer installations.

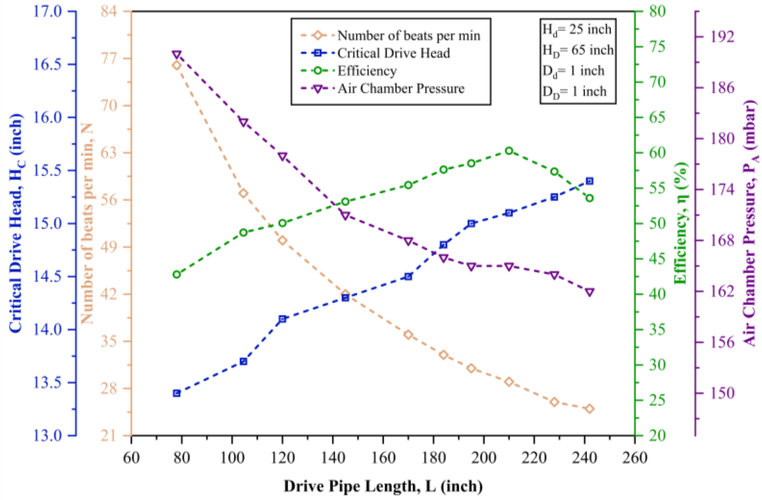

(a)

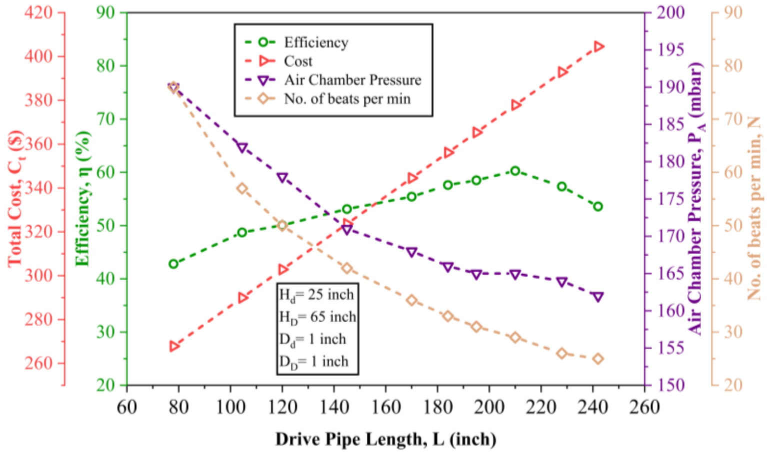

(b)

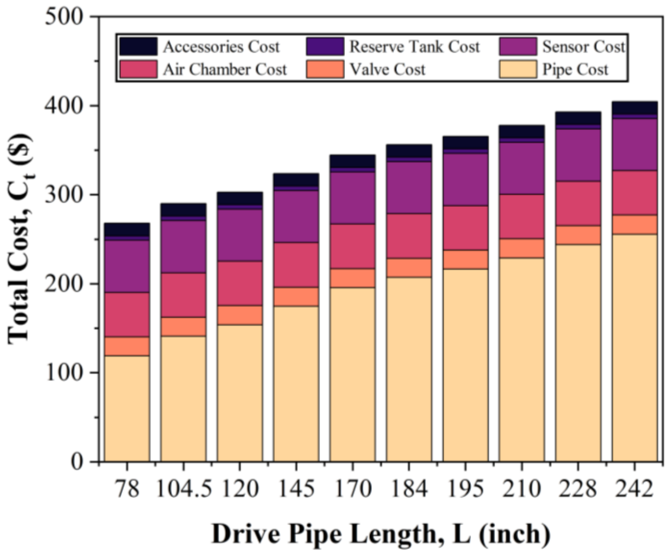

(c)

Figure 6: Effect of drive pipe length and delivery head on efficiency and total cost.

5.1.3 Effect of delivery head

Table 10 exhibits the results of variation in delivery head, H_D operating conditions proposed in **Table 4**. The table shows that the maximum η is 58.12% and it is found at the lowest head of 48 inches. After that, η decreases with an increase of H_D. Delivery head of 152 inches resulted in efficiency, η of 14.33%. The maximum H_C of 17.9 inches is observed at H_D 152 inches and the lowest of 13.8 inches at 48 inches. The lowest flow rate, Q_d is 0.116 L/min when the H_D is set to maximum and the highest is 2.105 L/min at the lowest H_D. C_t is calculated \$288.85 for H_D of 48 inches and \$375.55 for 152 inches.

Table 11: Experimental results of ram pump for variation of Delivery head

Design Case	Delivery Pipe Head, H_D (inch)	Critical Drive Head, H_C (inch)	Drive Pipe Flow rate, Q_s (L/min)	Waste Valve Flow rate, Q_w (L/min)	Delivery Pipe Flow rate, Q_d (L/min)	Efficiency, η (%)	Cost, C_t (\$)
1	48	13.8	6.954	5.849	2.105	58.12	288.85
2	51	13.8	6.883	4.971	1.912	56.67	291.35
3	65	14.1	6.742	5.444	1.298	50.06	303.05
4	86	15.3	6.256	5.382	0.874	48.05	320.55
5	95	15.5	6.246	5.578	0.668	40.64	328.05
6	111	15.9	5.870	5.406	0.460	34.79	341.35
7	123	16.3	5.793	5.450	0.343	29.13	351.35
8	136	16.5	5.146	4.915	0.231	24.42	362.15
9	145	17.0	5.060	4.882	0.178	20.40	369.65
10	152	17.9	4.920	4.804	0.116	14.33	375.55

Fig. 7(a) illustrates that η showed an exponential decreasing relationship with H_D, declining consistently from 58.12% at 48 inches to 14.33% at 152 inches. This is because when H_D increases, it requires extra energy to lift the water to a higher elevation against the gravitational force. For flow characteristics, Q_s decreases from 6.954 L/min to 4.92 L/min as H_D increases, representing a 29.2% reduction. More significantly, Q_d shows a dramatic decline from 2.105 L/min at 48 inches to only 0.116 L/min at 152 inches delivery head, representing a 94.5% reduction in useful water delivery. However, Q_w remains relatively stable, varying between 4.804 to 5.849 L/min, indicating consistent valve operation across different delivery conditions. The figure also states, H_C showed a steady increase from 13.8 inches to 17.9 inches as H_D increased from 48 to 152 inches. This trend aligns with theoretical expectations, as higher delivery heads require increased minimum driving pressure to initiate and maintain pump operation. **Fig. 7(a)** also indicates C_t demonstrated a linear increasing relationship with delivery head, rising from \$288.85 to \$375.55. This cost escalation primarily stems from the increased infrastructure requirements and energy losses associated with higher delivery configurations. In **Fig. 7(b)**, η exhibits an exponential decay relationship with increasing H_D, following the expected theoretical behavior where higher lifting requirements demand proportionally more energy input. The drive head-delivery head ratio (*h/H*) decreases from 0.521 to 0.1645 across the tested range, demonstrating the challenging operational conditions at higher delivery heads.

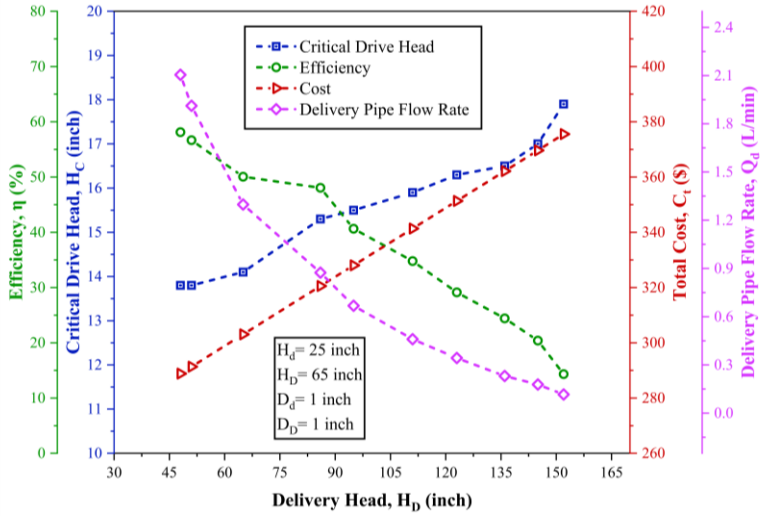

(a)

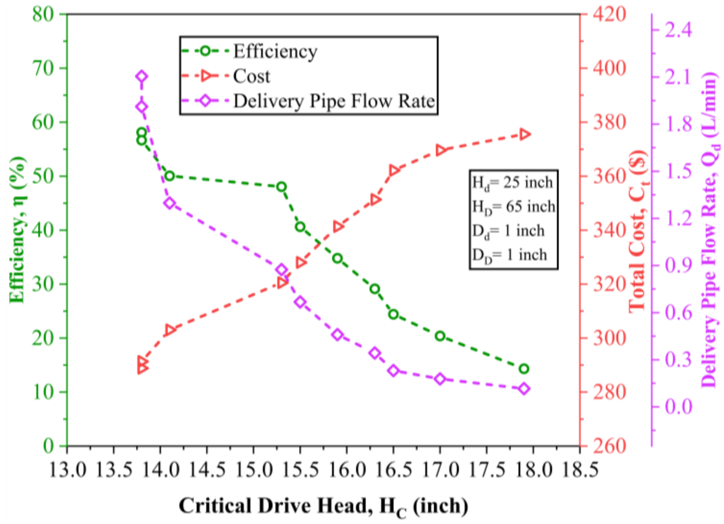

(b)

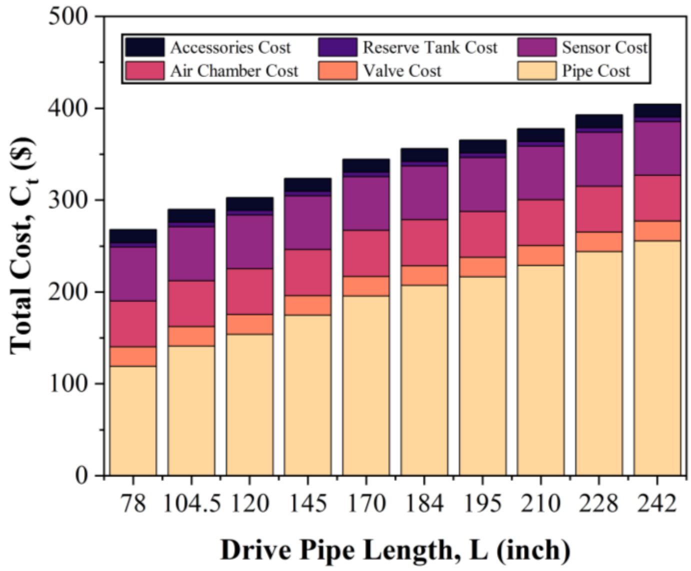

(c)

Figure 7: Effect of delivery head on efficiency and total cost.

In **Fig. 8,** the contour plot of the heatmap reveals a strong inverse relationship between H_D and η, with performance declining dramatically from 58.12% at 48-inch delivery head to 14.33% at 152-inch delivery head, representing a 75.3% efficiency reduction across the tested range. The efficiency contours demonstrate that optimal performance occurs at delivery heads below 70 inches with drive head-delivery head ratios (*h/H*) above 0.35. The Pearson correlation coefficient between H_D and η shows strong negative correlation (r = -0.90), confirming the inverse relationship observed in the visualization. H_C exhibits strong positive correlation with H_D (r = 0.85), increasing from 13.8 to 17.9 inches as H_D rises from 48 to 152 inches, a 30% increase in minimum operating requirements. The heatmap simultaneously shows C_t increasing linearly with H_D, rising from \$288.85 to \$375.55 across the tested range, a 30% cost escalation. This creates a double penalty scenario where higher delivery heads not only reduce efficiency but also increase capital investment. The cost gradient (shown in purple tones) indicates that every 10-inch increase in delivery head adds approximately \$8-12 to system cost, primarily due to additional piping materials and structural support requirements.

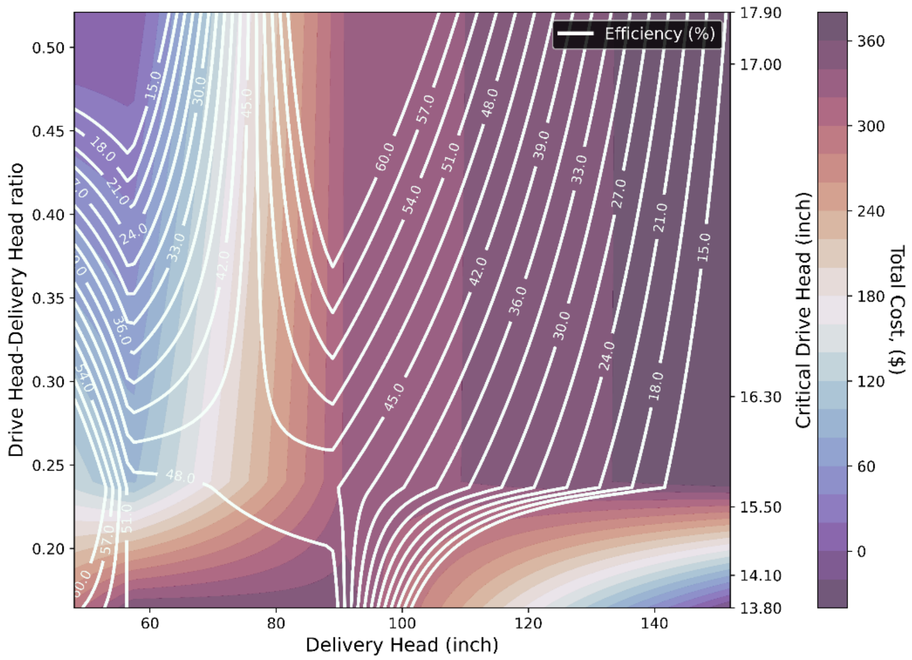

Figure 8: Effect of delivery head on efficiency and total cost.

5.1.4 Effect of air chamber volume

Table 11 illustrates the changes in efficiency, η, and cost as the V_A increases, as specified in **Table 4**. The highest efficiency, η, occurs in the 4th case when the volume is 3.09 L, while the lowest η is observed at 1.03 L. The maximum H_C is measured at the smallest volume, and the lowest value also occurs there. The maximum delivery flow rate, Q_d is recorded at a volume of 3.09 L, whereas the minimum flow rate of 1.227 L/min is in case 1. The C_t gradually rises with volume changes, with the highest and lowest costs recorded at 1.03 L and 5.35 L, respectively. The highest cost and lowest cost are recorded for 1.03L and 5.35L.

Table 12: Experimental results of ram pump for variation of Air chamber volume

Design Case	Air Chamber Volume, V_A (L)	Critical Drive Head, H_C (inch)	Drive Pipe Flow rate, Q_s (L/min)	Waste Valve Flow rate, Q_w (L/min)	Delivery Pipe Flow rate, Q_d (L/min)	Efficiency, η (%)	Cost. C_t ($)
1	1.03	16.4	7.112	5.885	1.227	44.86	267.8
2	1.61	15.9	6.961	5.666	1.295	48.37	275.6
3	2.06	15.1	6.699	5.401	1.298	50.38	281.7
4	3.09	14.8	6.75	5.40	1.350	52.0	295.6
5	3.71	15.2	6.742	5.444	1.298	50.06	303.9
6	4.53	16.0	7.037	5.695	1.342	49.58	315.05
7	5.35	16.3	7.152	5.857	1.295	47.08	326.1

Fig. 9(a) illustrates how varying the air chamber size influences several factors. It shows that η gradually improves from 44.86% to 52% as the V_A increases from 1.03L to 3.09L, then decreases to 47.08% at 5.35L. Between 1.03L and 3.09L, the air chamber better cushions hammer shocks, with compressed air acting like a spring that propels water through the pipe, boosting η. When the volume reaches 3.71L and above, the chamber becomes too large relative to the pipe, excessively damping pressure pulses and reducing η. The peak η is 52% at 3.09L. The H_C initially decreases and then begins to rise, peaking at 16.4 inches at 1.03L, decreasing to 14.8 inches (a 9.75% change), then increasing again to 16.3 inches at 5.35L. In the first four cases, the compressed air supplies enough force to push water, resulting in a lower head. Beyond 3.71L, the air is insufficiently compressed, requiring a higher drive head for operation. **Fig. 9(a)** also details the pipe's C_t and Q_d. The maximum flow rate is 1.35 L/min, achieved at 3.09 L of V_A. The C_t increases linearly from $267.80 to $326.10, a 21.76% increase. **Fig. 9(b)** shows the cost breakdown for different air chamber heights, with seven sizes resulting in varying costs. The pipe, accessories, reservoir tank, and valve costs remain unchanged. The lowest chamber cost is $13.90 at 1.03L, and the highest is $72.20 at 5.35L, with the total cost increasing by approximately 56% case.

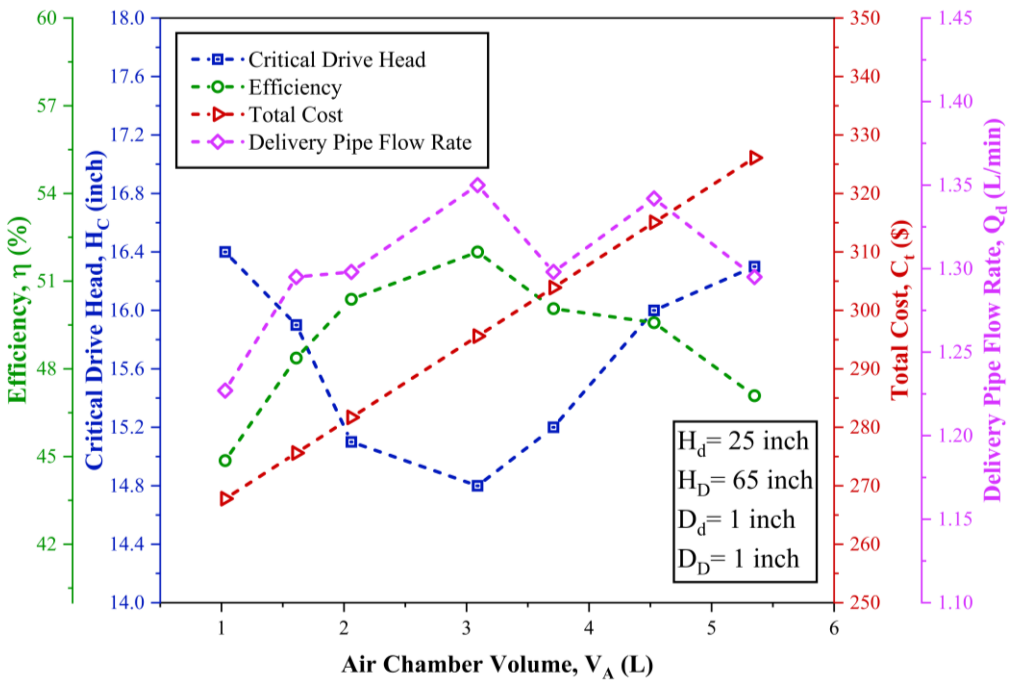

(a)

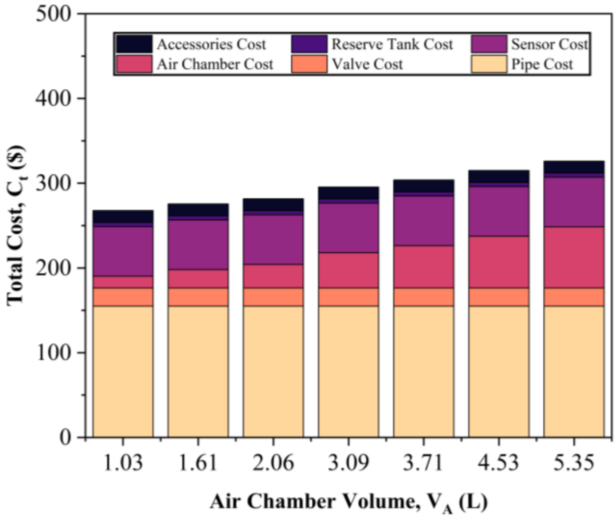

(b)

Figure 9: Effect of air chamber volume on efficiency and total cost

5.1.5 Effect of drive pipe length-drive pipe diameter ratio

The effect of drive pipe length-drive pipe diameter ratio in η from **Table 4** is derived. In **Table 12** the maximum and minimum η is recorded for L/D ratio of 195 and 242. The critical drive head, H_C is found maximum at 193.6 and minimum at 104 L/D ratio. The delivery pipe flow rate, Q_d is measured, and the maximum and minimum are recorded for a 104 and 193.6 ratio. Cost, C_t is also measured for all the ratios, and the lowest and highest amounts are identified in case 1 and case 12.

Table 13: Experimental results of ram pump for variation of Drive pipe length- Drive pipe Diameter

Design Case	Drive Pipe length, L (inch)	Drive Pipe Diameter, D (inch)	Drive Pipe length-Drive Pipe Diameter Ratio L/D	Critical Drive Head, H_C (inch)	Drive Pipe Flow rate, Q_s (L/min)	Waste Valve Flow rate, Q_w (L/min)	Delivery Pipe Flow rate, Q_d (L/min)	Efficiency, η (%)	Cost. C_t ($)
1	78	0.75	104	13.2	3.57	2.89	0.68	49.524	212.57
2	145	0.75	193.33	14.1	3.69	2.83	0.86	60.596	247.47
3	195	0.75	260	14.65	3.82	2.86	0.96	65.34	271.05
4	242	0.75	322.67	15.2	3.64	2.85	0.79	56.429	293.93
5	78	1.00	78	13.3	6.36	5.21	1.15	47.013	263.15
6	145	1.00	145	14.25	6.72	5.24	1.48	57.262	323.85
7	195	1.00	195	14.8	6.69	5.00	1.59	61.794	364.85
8	242	1.00	242	15.4	6.57	5.19	1.38	54.612	404.65
9	78	1.25	62.40	14.5	9.05	7.51	1.54	44.24	331.30
10	145	1.25	116	16.2	9.37	7.49	1.88	52.166	422.35
11	195	1.25	156	19.1	9.88	7.65	2.23	58.684	483.85
12	242	1.25	193.6	21.4	9.72	7.80	1.92	51.36	543.55

Fig. 10(a) illustrates how η varies with different L/D ratios. In cases 1 to 4, the drive pipe diameter remains at 0.75 inch, but L increases. The η rises from 49.524% to 65.34% as the L/D ratio goes from 104 to 260. After reaching the peak of 65.34%, it decreases to 56.42% at an L/D ratio of 322.67. As the drive pipe length increases with the same diameter, increased friction causes η to sharply decline. In cases 5 to 8, the diameter is 1 inch; in cases 8 to 12, it is 1.25 inches. These regions show similar η patterns. Overall, the highest η of 65.34% occurs at a length of 195 inches and diameter of 0.75 inch. The peaks for other regions are 61.794% and 58.684% respectively, indicating that η tends to decrease as the pipe diameter increases. In this experiment, the drive head and energy are constant. Larger diameters allow more water flow, but since the lifting energy remains fixed, η drops. The H_C increases with both D and L, with a maximum of 21.4 inches at an L/D ratio of 193.6, and a minimum of 13.2 inches at an L/D of 104, a 62.12% increase. More flow requires more external pressure from the drive head. **Fig. 10(a)** also shows C_t at different ratios; costs rise linearly across all three regions. The lowest C_t is \$212.57 at an L/D ratio of 104, and the highest is \$543.55 at 193.6 ratio. The maximum pipe length is 242 inches with the largest diameter, which increases C_t. **Fig. 10(b)** depicts the Q_d behaviour, which increases to a peak before slightly decreasing. This pattern mirrors the η decline discussed earlier. The maximum rate is 2.23L for the 1.25- inch diameter cases. Flow rate increases with diameter, with a first- region peak of 0.96 L/min and a second-region peak of 1.59 L/min, showing gradual growth. As the diameter increases, more water flows through the pipe, raising the flow rate by 132.29%. **Fig. 10(c)** breaks down C_t, showing that expenses for the air chamber, reservoir tank, and sensors stay consistent. Variations in total cost stem from different pipe sizes and accessories; at an L/D ratio of 193.6, pipe costs reach \$383.7, making it the highest costs.

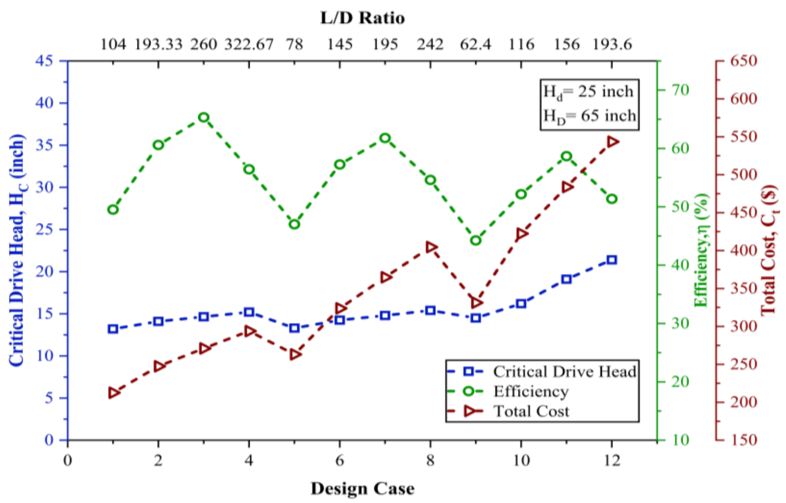

(a)

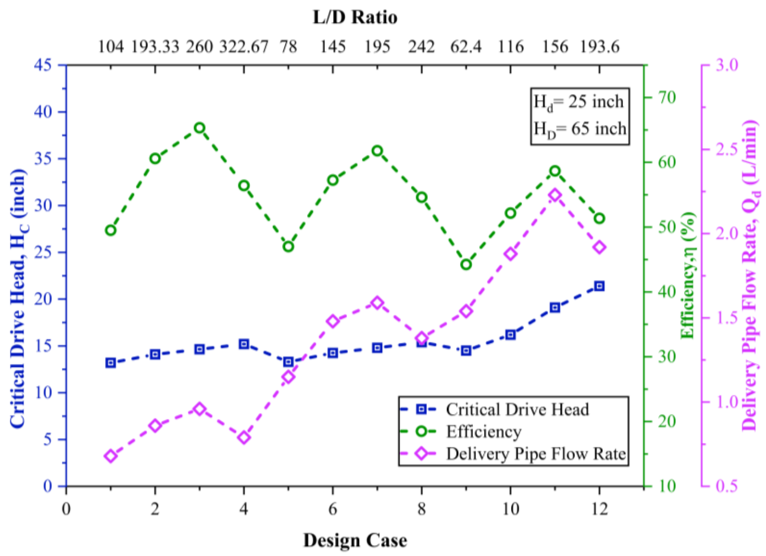

(b)

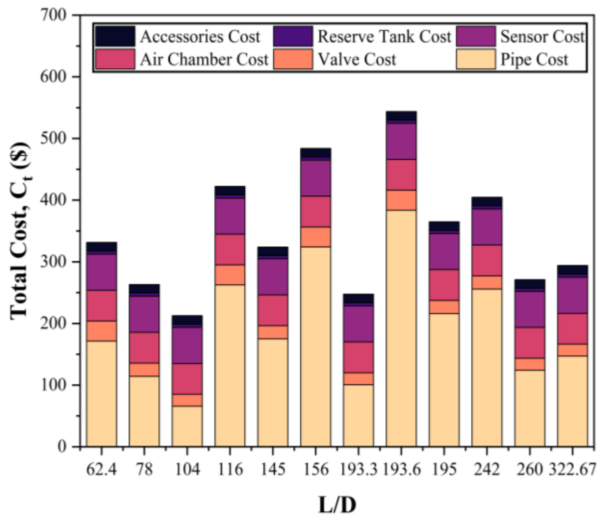

(c)

Figure 10: Effect of drive pipe length-drive pipe diameter ratio on efficiency and total cost.

Fig. 11 demonstrates the relationships among drive pipe length, diameter, critical drive head, and cost. Drive pipe length is notably correlated with H_C and C_t (r = 0.59), meaning that increasing the length by 1 unit leads to about a 59% increase in both metrics. A length, L of 78 inches achieves an η of 49.52%, while 195 inches yields 65.34%. The η contour shows a moderate positive correlation (r = 0.48) with L. The L/D ratio correlates strongly with L (r = 0.89). The correlation between L/D ratio and η is positive (r= 0.44), but only weakly related to C_t (r = 0.11), indicating that the trade-off between ratio and C_t is minimal. The η and total cost trade-off is approximately 21%. Drive pipe diameter, D strongly correlates with drive flow rate, Q_s (r = 0.94) and delivery pipe flow rate, Q_d (r= 0.85). For example, a 0.75-inch pipe's flow rate is 3.57 L/min, increasing to 9.72 L/min for 1.25 inches. Likewise, delivery flow rate varies from 1.92 L/min to 0.68 L/min.

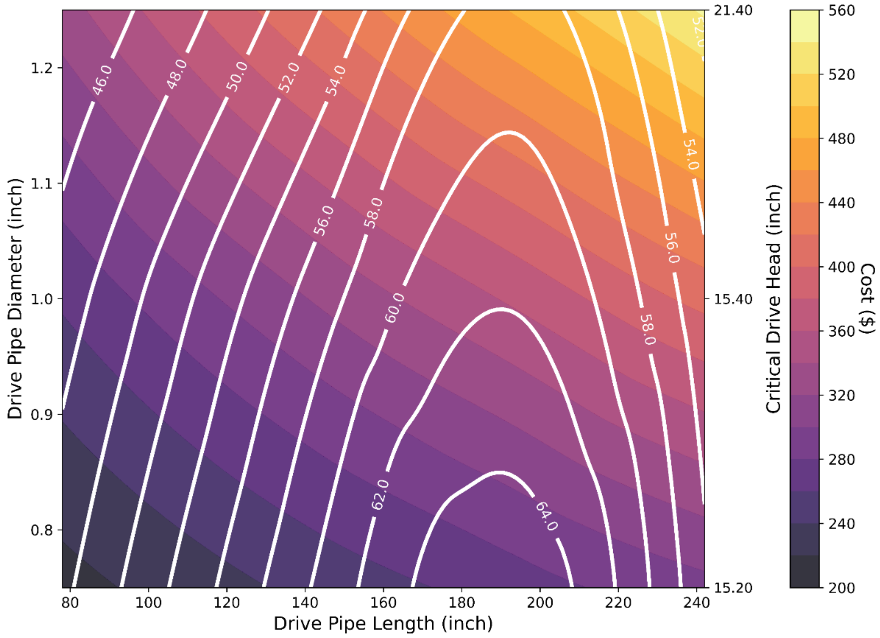

Figure 11: Effect of drive pipe length-drive pipe diameter ratio on efficiency and total cost.

5.2 Response surface regression analysis

Response surface regression is a statistical method used to ascertain a non-linear relationship between input and output variables. This research employs this paradigm to express the output parameters as quadratic functions of the selected variables. Quadratic regression offers much greater predictive accuracy than linear regression models in predicting pump's performance [39]. The outputs are anticipated to have a minimal residual within the specified operating range of the decision variables. RSM was implemented using Python's scikit-learn library to develop quadratic empirical equations for all output parameters. The polynomial feature expansion with degree 2 was applied to transform the original five input variables into a 20-dimensional feature space comprising linear terms (5), quadratic terms (5), and interaction terms (10). The expanded design matrix was fitted using ordinary least squares regression to generate second-order polynomial equations. The quadratic functions obtained from the regression analysis are defined below.

$$\eta = 62.422457 + 0.016742 \times L - 0.000210 \times D_d - 0.003198 \times D_D - 0.009056 \times H_D + 0.000162 \times V_A - 0.001239 \times L^2 + 0.005178 \times L \times D_d + 0.054161 \times L \times D_D + 0.001488 \times L \times H_D + 0.081529 \times L \times V_A - 6.046000 \times {D_d}^2 - 0.003303 \times D_d \times D_D - 0.022735 \times D_d \times H_D - 0.000619 \times D_d \times V_A - 0.004797 \times {D_D}^2 - 0.216932 \times D_D \times H_D - 0.011703 \times D_D \times V_A - 0.001185 \times {H_D}^2 - 0.023083 \times H_D \times V_A - 1.245154 \times {V_A}^2$$

$$H_C = 10.079500 - 0.028767 \times L - 0.013103 \times D_d + 0.001002 \times D_D + 0.015615 \times H_D + 0.000312 \times V_A + 0.000006 \times L^2 + 0.061603 \times L \times D_d - 0.028113 \times L \times D_D + 0.003981 \times L \times H_D - 0.069240 \times L \times V_A + 25.700000 \times {D_d}^2 - 0.005550 \times D_d \times D_D - 0.836068 \times D_d \times H_D - 0.048299 \times D_d \times V_A + 0.001502 \times {D_D}^2 + 0.080719 \times D_D \times H_D + 0.004028 \times D_D \times V_A + 0.000036 \times {H_D}^2 + 0.078236 \times H_D \times V_A + 0.504101 \times {V_A}^2$$

$$Q_d = 0.942606 + 0.00435 \times L + 0.000704 \times D_d + 0.000019 \times D_D - 0.002357 \times H_D - 0.000065 \times V_A - 0.000038 \times L^2 + 0.004040 \times L \times D_d - 0.000032 \times L \times D_D - 0.000390 \times L \times H_D + 0.008278 \times L \times V_A - 0.68000 \times {D_d}^2 + 0.000371 \times D_d \times D_D + 0.043432 \times D_d \times H_D + 0.002548 \times D_d \times V_A + 0.000028 \times {D_D}^2 - 0.001130 \times D_D \times H_D + 0.000005 \times D_D \times V_A + 0.000192 \times {H_D}^2 - 0.012993 \times H_D \times V_A - 0.021156 \times {V_A}^2$$

$$C_t = 53.417492 - 0.23430 \times L - 0.062543 \times D_d + 0.002404 \times D_D + 0.127019 \times H_D + 0.004625 \times V_A - 0.0002828 \times L^2 + 1.591787 \times L \times D_d - 0.098473 \times L \times D_D + 0.012495 \times L \times H_D - 0.314271 \times L \times V_A + 186.140000 \times {D_d}^2 - 0.028867 \times D_d \times D_D - 3.938294 \times D_d \times H_D - 0.227411 \times D_d \times V_A + 0.003607 \times {D_D}^2 + 0.283310 \times D_D \times H_D + 0.013546 \times D_D \times V_A - 0.000025 \times {H_D}^2 + 0.771863 \times H_D \times V_A + 0.182864 \times {V_A}^2$$

The model's accuracy was assessed using a random data set and compared to the experimental results, while several error matrices were computed for the derived model. The MAPE, *R*2, MAE and RMSE metrics for all three output functions are within the acceptable range, indicating a strong fit between the quadratic equations and the experimental model. This indicates that these equations effectively characterize the model's behavior and are appropriate for predictive applications. The results of the error assessment are illustrated in **Table 13**. Then, **Fig. 12** shows a comparison of the predicted values from the RSM model with the actual measured values for various parameters. The red dashed line is the "Perfect Prediction" line, where the predicted values would be equal to the actual values. Correlation coefficients indicate the strength of the relationship between actual and predicted values. Higher values (close to 1) represent better model accuracy.

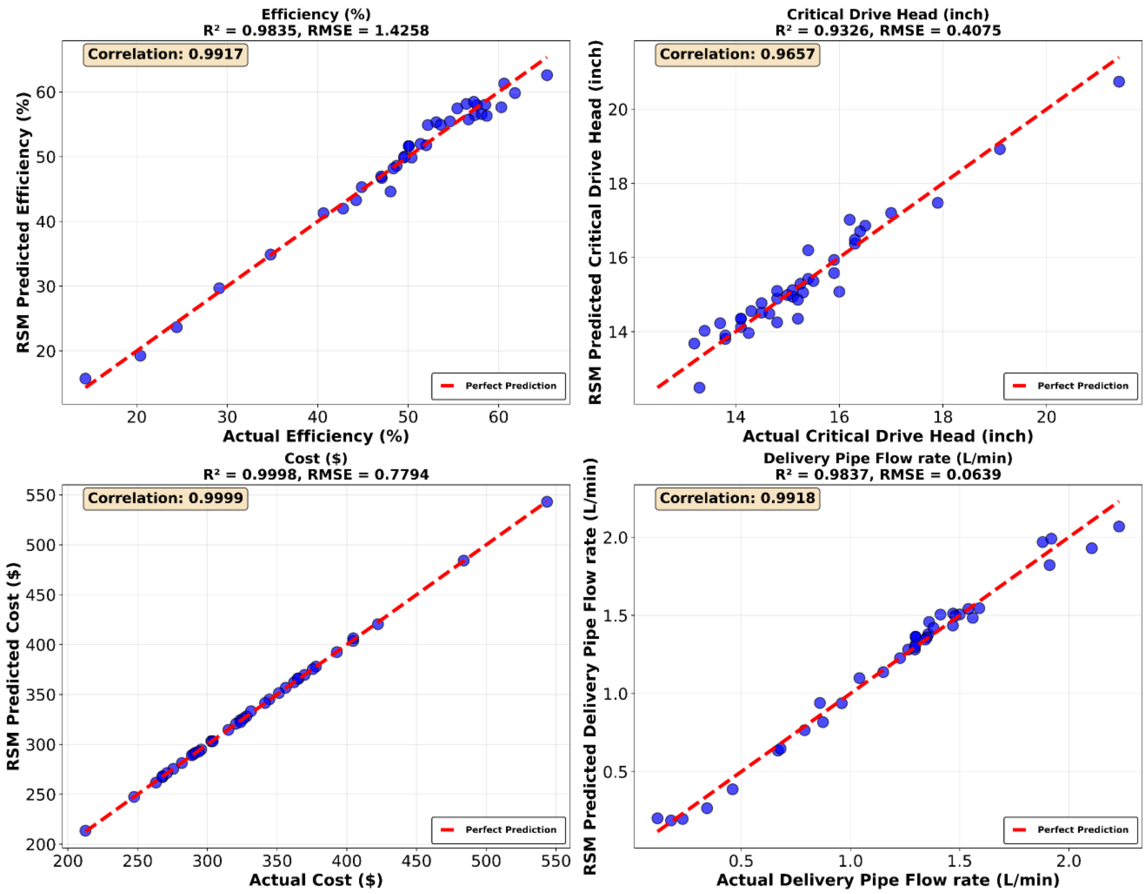

Figure 12: Illustration of predicted and actual values from RSM model.

Table 14: Error Assessment of the RSM Model.

Criteria	R^2	RMSE	MAE	MAPE (%)
Efficiency (%)	0.9835	1.4258	1.1443	2.47
Critical Drive Head (inch)	0.9326	0.4075	0.3099	2.03
Cost ($)	0.9998	0.7794	0.5675	0.17
Delivery Pipe Flow rate (L/min)	0.9837	0.0639	0.0493	6.45

5.3 Ensemble model analysis

To enhance prediction accuracy and capture complex nonlinear relationships, a hybrid ensemble model combining ANN, XGBoost and RSM was developed. This hybrid approach leverages the strengths of each method to achieve superior predictive performance. A feedforward artificial neural network was developed using TensorFlow/ Keras with five hidden layers (128, 64, 32, 16 neurons) and ReLU activation functions. The Adam optimizer (learning rate=0.001) was employed for gradient-based optimization with batch normalization and dropout regularization (0.3, 0.2, 0.1) to prevent overfitting. Early stopping with 50-epoch patience was implemented based on validation loss monitoring.

Extreme Gradient Boosting (XGBoost) was employed as a tree-based ensemble method utilizing second-order gradient information (Newton-Raphson optimization) for superior predictive performance. The regressors were trained with the following hyperparameters: 100 estimators, maximum depth of 5, learning rate of 0.1, and regularization through subsampling (0.8) and feature sampling (0.8). Individual XGBoost regressors were trained for each output parameter (efficiency, critical drive head, cost, flow rate) using the MultiOutputRegressor wrapper to handle the multi-target regression problem effectively.

A weighted ensemble approach combined predictions from RSM (20%), ANN (40%), and XGBoost (40%) models. Output constraints were applied using numpy clipping to ensure predictions remained within experimental ranges. The ensemble framework incorporated multi-objective Pareto optimization with constrained search space generation to identify optimal HRP configurations. **Table 14** depicts the error assessment of the ensemble model**.**

The three-dimensional response surfaces presented in **Fig. 13** illustrate the complex interdependencies between key HRP performance parameters. These surfaces were generated using predictions from the weighted enhanced ensemble model. The visualization employs Radial Basis Function interpolation with multiquadric kernels applied to 100,000 constrained candidate solutions, ensuring all data points adhere to experimentally validated parameter ranges. Gaussian smoothing (σ=1.0-1.5) was applied to enhance surface continuity while preserving critical performance trends. **Fig. 13(a)** demonstrates the relationship between efficiency, critical drive head, and delivery flow rate, revealing peak efficiency zones (>60%) at moderate critical drive heads (15-17 inches) and higher flow rates (1.5-2.0 L/min). **Fig. 13(b)** presents the efficiency-cost-critical drive head relationship, indicating that optimal efficiency (60-65%) is achievable at moderate costs ($300-400) with lower critical drive heads (14-16 inches).

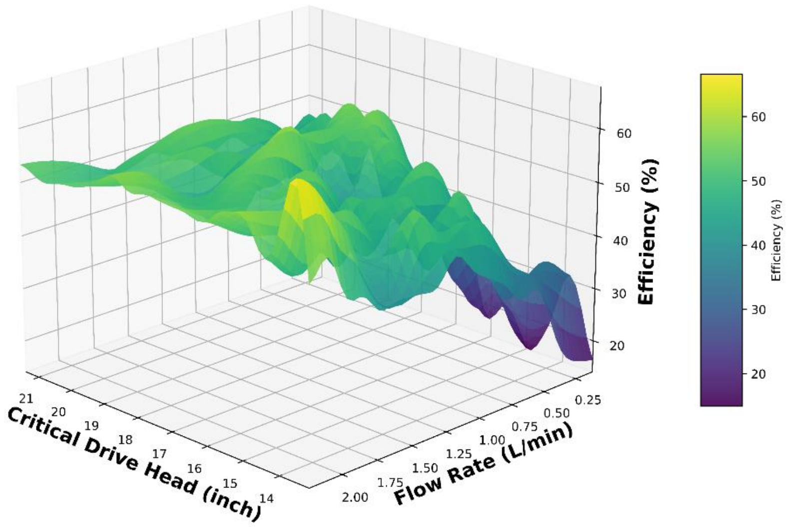

(a)

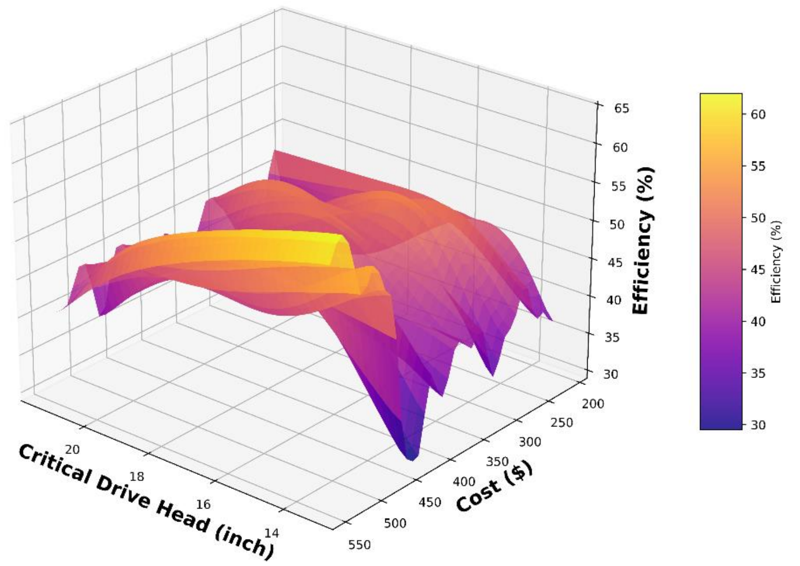

(b)

Figure 13: Illustration of predicted and actual values from RSM model.

Table 15: Error Assessment of the Ensemble Model.

Criteria	R^2	RMSE	MAE	MAPE (%)
Efficiency (%)	0.9705	1.9063	1.4923	3.39
Critical Drive Head (inch)	0.8802	0.5434	0.4496	2.88
Cost ($)	0.9903	6.2151	5.0080	1.53
Delivery Pipe Flow rate (L/min)	0.9655	0.0930	0.0761	11.29

5.4 Sensitivity analysis

A Pearson correlation coefficient matrix was produced using the regression model to examine the correlations among input design parameters and output performance metrics. The sensitivity analysis results are visualized in a correlation heatmap as shown in **Fig. 14**, indicating the extent of sensitivity of output parameters to variations in input parameters. Higher correlation coefficient values suggest stronger sensitivity, while positive or negative signs reveal direct or inverse proportional relationships. The correlation analysis demonstrates that Efficiency (η) shows strong negative correlation with delivery head (H_D) and moderate positive correlation with drive pipe length (L). Critical drive head (H_C) exhibits strong positive correlation with delivery head (H_D) and moderate correlation with drive pipe diameter (D_d). Total cost (C_t) is significantly correlated with drive pipe length (L) and drive pipe diameter (D_d). Delivery flow rate (Q_d) shows moderate positive correlation with efficiency and inverse correlation with delivery head. Among all input parameters, delivery head (H_D) and drive pipe length (L) exhibit the highest degrees of correlation with the performance metrics, indicating these are the most critical design parameters for system optimization.

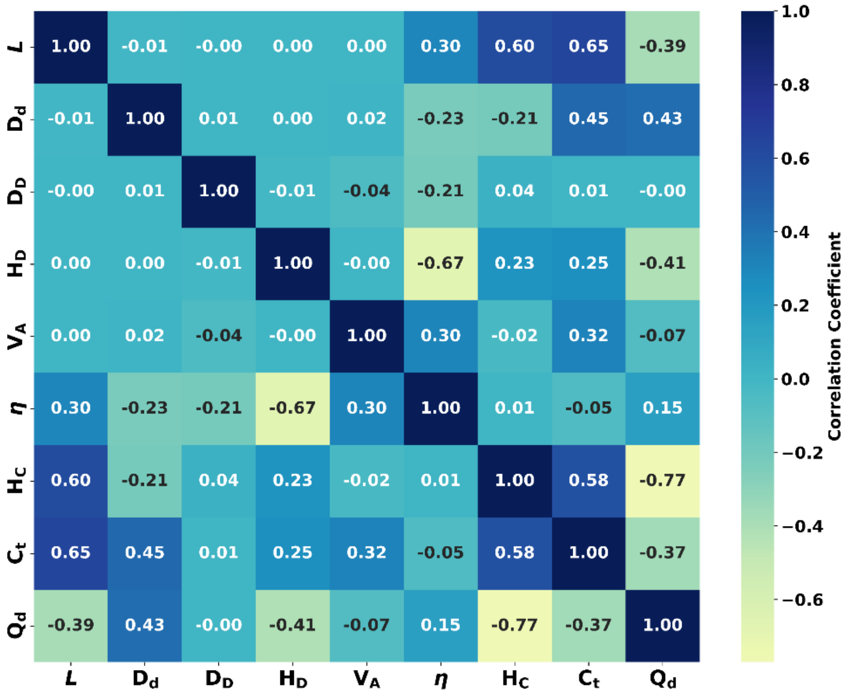

Figure 14: Heatmap illustration of correlation matrix showing the impact of each input parameter on the outputs

So, further emphasis should be given to these 2 design parameters. **Fig. 15** shows how much each output changes when L and H_D is changed. In **Fig. 15(b)** shows H_D emerged as the most influential parameter on system efficiency, exhibiting a sensitivity of ±15.09% (30.17% total range). The critical drive head sensitivity was ±3.54 inches, while cost varied by ±\$61.47. Notably, the relative sensitivity analysis identified flow rate as the most sensitive output to delivery head variations (relative sensitivity: 1.790), indicating strong hydraulic coupling. **Fig. 15(a)** L ranked second in efficiency impact with ±6.29% sensitivity (12.57% total range). Extending the drive pipe from 78 to 242 inches enhanced the water hammer effect, improving energy transfer efficiency. This parameter showed the highest cost sensitivity at ±\$84.55, reflecting the material costs associated with pipe length modifications. The critical drive head varied by ±3.45 inches across the range, demonstrating moderate operational flexibility. This sensitivity analysis provides actionable design guidelines for field deployment. For high-head applications (>100 inches), the 30.17% efficiency variation range emphasizes the critical importance of minimizing delivery head through appropriate site selection and system placement.

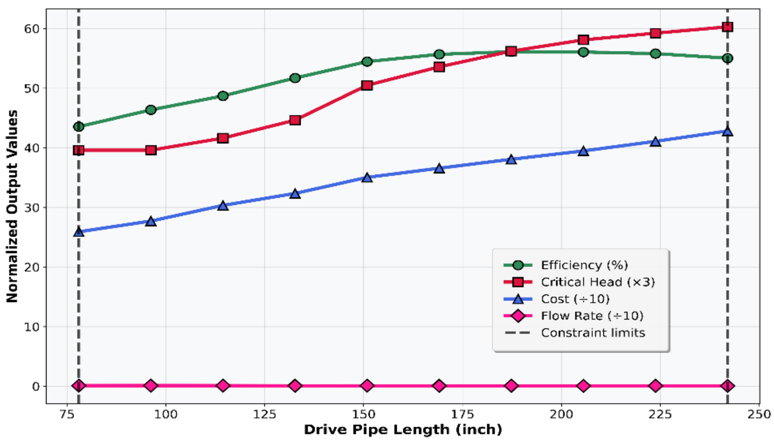

(a)

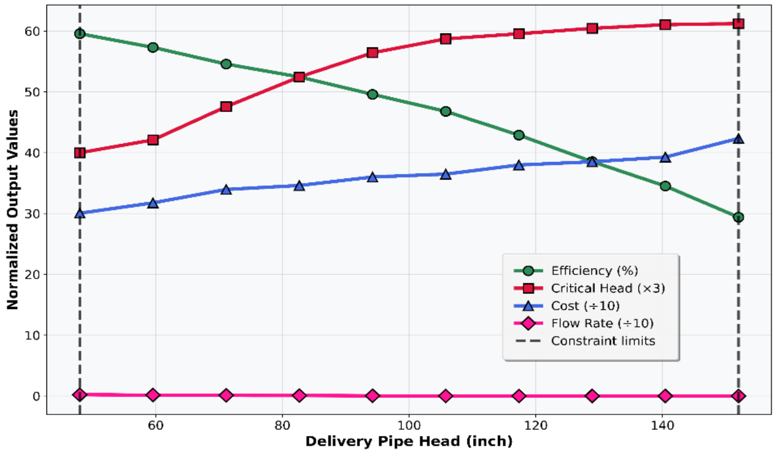

(b)

Figure 15: Sensitivity analysis plots showing the impact of Length and Drive Head on the outputs.

5.5 Optimal design conditions

The multi-objective optimization successfully identified ten optimal design configurations representing the best trade-offs between maximizing efficiency (η) and delivery flow rate (Q_d) while minimizing critical drive head (H_C) and total cost (C_t). Table 15 presents the Pareto-optimal solutions obtained through the weighted ensemble model optimization.

Rank	Drive Pipe Length, L (inch)	Drive Pipe Diameter, D_d (inch)	Delivery Pipe Diameter, D_D (inch)	Delivery Pipe Head, H_D (inch)	Air Chamber Volume, V_A (L)	Efficiency, η (%)	Critical Drive Head, H_C (inch)	Total Cost, C_t ($)	Delivery Pipe Flow rate, Q_d (L/min)	Fitness Score
1	209.72	0.75	0.75	49.32	5.29	61.34	13.6	232.271	2.23	0.55
2	112.63	0.75	0.5	49.61	3.66	59.966	13.2	213.828	1.437	0.473652
3	118.31	0.75	0.75	48.66	3.41	59.286	13.2	212.57	1.372	0.472311
4	120.44	0.75	0.5	48.49	3.1	60.007	13.2	212.57	1.229	0.46265
5	117.97	0.75	0.5	48.77	3.17	59.594	13.2	212.57	1.27	0.462047
6	178.65	0.75	0.5	48.09	3.2	60.303	13.4	225.713	1.395	0.460151
7	125.18	0.75	0.75	50.87	3.23	59.6	13.2	213.477	1.292	0.451442
8	103.57	0.75	0.5	48.12	3.83	58.5	13.2	213.54	1.415	0.450922
9	114.37	0.75	0.75	49.79	3.71	58.341	13.3	218.72	1.432	0.437112
10	114.1	0.75	0.5	48.33	3.99	59.27	13.2	219.55	1.633	0.419552

Table 16: Results of Multi-objective optimization for maximum η and Qd, minimum Hc and Ct

The highest-ranking configuration shown in **Fig. 16** achieved optimal performance with drive pipe length of 209.72 inches, 0.75-inch drive pipe diameter, 0.75-inch delivery pipe diameter, 49.32-inch delivery head, and 5.29 L air chamber volume, delivering 61.34% efficiency, 13.6-inch critical drive head, $232.27 total cost, and 2.23 L/min delivery flow rate. The 209.72-inch drive pipe length falls near the theoretical optimum identified in the parametric analysis (210 inches), where water hammer effects are maximized while friction losses remain manageable. The 0.75-inch pipe diameter provides the ideal balance between flow velocity and pressure drop, creating sufficient momentum for effective valve closure, while the relatively large air chamber volume (5.29 L) ensures adequate pressure dampening and energy storage, converting kinetic energy to potential energy efficiently. The low delivery head (49.32 inches) minimizes gravitational work requirements, allowing more energy to be available for pumping.

The optimization revealed several critical trade-offs inherent in hydraulic ram pump design. Seven out of ten optimal solutions utilize 0.75-inch drive pipe diameter, indicating this diameter provides the optimal balance between flow area and velocity for the given operational range, while delivery heads cluster around 48-51 inches, representing the sweet spot for gravitational lift versus pumping efficiency. The efficiency versus cost trade-off demonstrates that achieving higher efficiency (59.3-61.34%) requires increased investment in larger air chambers and longer drive pipes, resulting in costs ranging from $212.57 to $232.27, reflecting the physical reality that optimal water hammer effects require precise geometric proportions and adequate energy storage capacity. The top-ranked solution achieves the highest delivery flow rate (2.23 L/min) while maintaining a moderate critical drive head (13.6 inches) through an optimal L/D ratio of 279.6, which maximizes pressure surge generation while maintaining operational reliability across seasonal water level variations. Critical drive heads ranging from 13.2-13.6 inches across top solutions ensure reliable operation with minimal seasonal adjustments, establishing quantitative design principles for cost-effective HRP implementation in rural water supply applications.

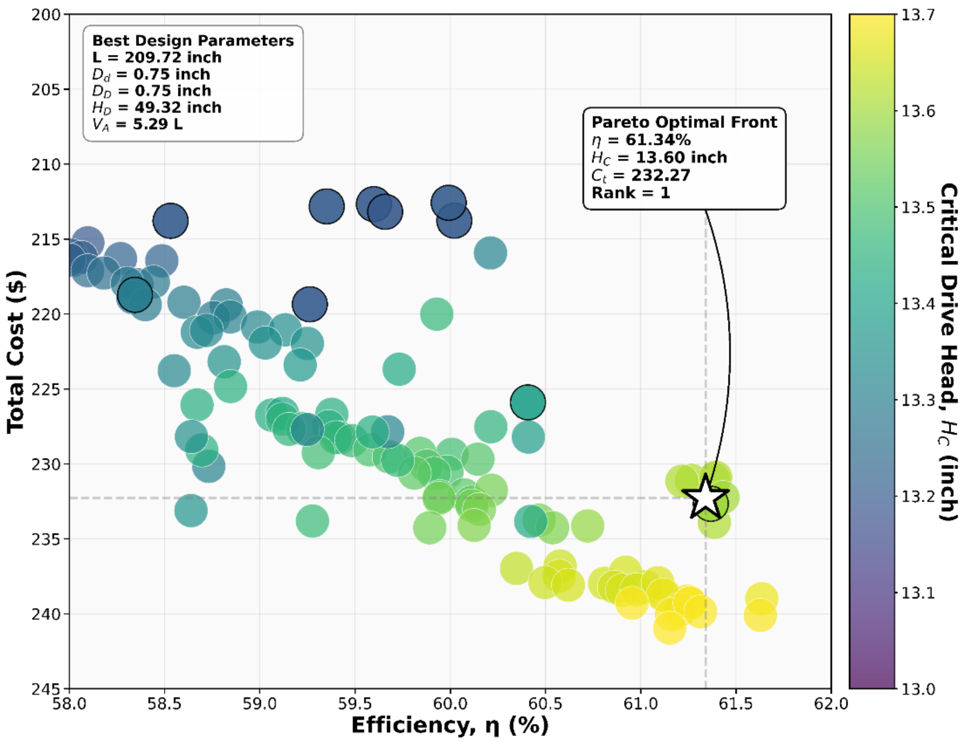

Figure 16: Selection of the optimal point from the pareto optimal solution set.

Chapter 6: Conclusion

6.1 Conclusion

This study provides a comprehensive investigation of a Hydraulic Ram Pump (HRP) for sustainable water lifting in rural and off- grid areas, combining experimental, analytical, and optimization methods. A combined approach using controlled laboratory tests, theoretical models, and a hybrid ensemble machine learning framework (ANN–XGBoost–RSM) was employed to assess and optimize the system's efficiency, flow rate, drive head, and cost. The main aim was to maximize hydraulic efficiency and flow while reducing drive head and overall costs. The best experimental results were achieved at an L/D ratio of 260 (195- inch drive pipe length, 0.75- inch diameter), reaching an efficiency of 65.34%. Multi- objective optimization identified an optimal setup with 61.34% efficiency, a flow rate of 2.23 L/min, a drive head of 13.6 inches, and a total cost of approximately $232.27. Parametric analysis showed that drive pipe length has a non- linear relationship with efficiency, increasing to an optimum before decreasing due to friction. Delivery head is strongly inversely related to efficiency ($r = -0.90$) and flow rate, indicating that lower heads improve performance. Air chamber volume has an optimal range (~3.09L); exceeding this reduces efficiency due to over- damping. Critical drive head correlates strongly with geometric and operational parameters, increasing with drive pipe length ($r = 0.90$), delivery head ($r = 0.85$), and pipe diameter, but negatively with the h/L ratio ($r = -3.52$). This highlights the importance of proportional design to mitigate seasonal performance issues. Cost analysis shows piping components account for 50.5 - 65.9% of total costs, which scale linearly with pipe length and diameter. A significant negative correlation ($r = -65.9$) between efficiency and cost reflects a trade-off: marginal efficiency improvements sbeyond the optimum lead to much higher expenses. Overall, the results establish quantitative relationships between performance and cost, providing practical design benchmarks. The guidelines balance hydraulic efficiency and economic feasibility, supporting the development of cost- effective, sustainable, and low- maintenance water supply solutions for rural and domestic use.

6.2 Recommendation for future works

While this study provides comprehensive insights into HRP optimization and critical drive head characterization, several avenues warrant further investigation to advance the technology's practical deployment and theoretical understanding.

The experimental scope was constrained to a single waste valve geometry and CPVC piping material. Future research should systematically investigate alternative valve designs—including conical, hemispherical, and aerodynamic profiles with varying orifice diameters, stroke lengths, and spring stiffness—to identify geometries that minimize pressure losses while maintaining reliable closure dynamics. Additionally, comparative analysis of alternative pipe materials such as HDPE, stainless steel, and composite materials would elucidate the influence of pipe elasticity, surface roughness, and thermal expansion on water hammer propagation and long-term performance degradation under continuous cyclic loading conditions.

The ensemble machine learning model demonstrated strong predictive capability, yet its training was limited to 39 experimental data points augmented by synthetic samples. Expanding the experimental dataset to encompass broader parameter spaces and extreme operational conditions would enhance model robustness. Integration of physics-informed neural networks that embed governing hydraulic equations as constraints could further improve prediction accuracy while reducing data requirements. Moreover, the optimization framework should incorporate additional practical criteria such as noise levels, installation complexity, and maintenance accessibility through multi-criteria decision analysis weighted according to stakeholder preferences.

Field validation remains a critical gap. The laboratory setup operated under controlled conditions with stable water supply and minimal contamination. Deploying prototype systems in actual rural settings would reveal performance degradation mechanisms arising from sediment accumulation, seasonal water quality variations, and ambient temperature fluctuations. Long-term field trials spanning multiple hydrological seasons are essential to validate the predicted maintenance intervals and operational reliability under real-world conditions.

Finally, investigating series and parallel multi-pump arrangements could unlock performance improvements unattainable with individual units, particularly for high-head or high-flow applications. Hybrid systems integrating HRP with solar-powered backup pumps warrant exploration to ensure water supply continuity during low-flow periods. Addressing these recommendations would advance hydraulic ram pump technology toward widespread adoption, providing sustainable water access solutions for underserved communities globally.

References

[1] K. Chartzoulakis and M. Bertaki, "Sustainable Water Management in Agriculture under Climate Change," *Agriculture and Agricultural Science Procedia*, vol. 4, pp. 88–98, 2015, doi: 10.1016/j.aaspro.2015.03.011.

[2] Prof. C. C. Handa, "Development of Hydraulic Ram Pump for Agriculture Uses and Approach A Review," *Int J Res Appl Sci Eng Technol*, vol. 11, no. 5, pp. 3133–3136, May 2023, doi: 10.22214/ijraset.2023.52277.

[3] S. Ndache MOHAMMED, "Design and Construction of a Hydraulic Ram Pump from Leonardo Electronic Journal of Practices and Technologies," *Leonardo Electronic Journal of Practices and Technologies*, pp. 59–70, 2007.

[4] P. Diwan, "DESIGN AND FABRICATION OF HYDRAULIC RAM WITH METHODS OF IMPROVING EFFICIENCY," 2016, Accessed: Aug. 18, 2025. [Online]. Available: https://www.researchgate.net/publication/372658169_DESIGN_AND_FABRICATION_OF_HYDRAULIC_RAM_WITH_METHODS_OF_IMPROVING_EFFICIENCY

[5] S. Yannopoulos *et al.*, "Evolution of Water Lifting Devices (Pumps) over the Centuries Worldwide," *Water (Basel)*, vol. 7, no. 9, pp. 5031–5060, Sep. 2015, doi: 10.3390/w7095031.

[6] R. R. Huiswoud, "CORN GROWING IN SURINAM," *Caribbean Food Crops Society* , 1969, doi: doi.org/10.22004/ag.econ.263510.

[7] Shamsudeen A. Sodangi, "Review of Hydraulic Ram Pumps (Hydram) and Recommendations for Revival," *International Journal of Trend in Scientific Research and Development (IJTSRD)*, vol. 6, no. 6, pp. 1078–1084, 2022, Accessed: Aug. 18, 2025. [Online]. Available: https://www.ijtsrd.com/papers/ijtsrd51959.pdf

[8] M. Suarda, A. Ghurri, M. Sucipta, and I. G. B. W. Kusuma, "Investigation on characterization of waste valve to optimize the hydraulic ram pump performance," 2018, p. 020023. doi: 10.1063/1.5046607.

[9] M. Suarda, M. Sucipta, and I. G. K. Dwijana, "Investigation on flow pattern in a hydraulic ram pump at various design and setting of its waste valve," *IOP Conf Ser Mater Sci Eng*, vol. 539, no. 1, p. 012008, Jun. 2019, doi: 10.1088/1757-899X/539/1/012008.

[10]J. Li *et al.*, "Structural design and parameter optimization on a waste valve for hydraulic ram pumps," *Proceedings of the Institution of Mechanical Engineers, Part A: Journal of Power and Energy*, vol. 235, no. 4, pp. 747–765, Jun. 2021, doi: 10.1177/0957650920967489.

[11]A. Johanis, R. Mado, and H. Dida, "Effect of Waste Valve Tuning on Hydraulic Ram Pump Efficiency," in *Proceedings of the 4th International Conference on Applied Science and Technology on Engineering Science*, SCITEPRESS - Science and Technology Publications, 2021, pp. 237–242. doi: 10.5220/0010943000003260.

[12]B. W. Young, "Design of Hydraulic Ram Pump Systems," *Proceedings of the Institution of Mechanical Engineers, Part A: Journal of Power and Energy*, vol. 209, no. 4, pp. 313–322, Nov. 1995, doi: 10.1243/PIME_PROC_1995_209_010_01.

[13]H. N. Najm, P. H. Azoury, and M. Piasecki, "Hydraulic ram analysis: a new look at an old problem," *Proceedings of the Institution of Mechanical Engineers, Part A: Journal of Power and Energy*, vol. 213, no. 2, pp. 127–141, Mar. 1999, doi: 10.1243/0957650991537491.

[14]A. M. Sharma, C. A. Ragsdale, U. P. Nwali, and S. B. Pidugu, "Performance of a Modified

Ram Pump With Double Inlets: An Innovative Technique to Improve Performance of the Hydraulic Ram Pump," in *Volume 8: Energy*, American Society of Mechanical Engineers, Nov. 2020. doi: 10.1115/IMECE2020-23626.

[15]X. Guo *et al.*, "Optimal design and performance analysis of hydraulic ram pump system," *Proceedings of the Institution of Mechanical Engineers, Part A: Journal of Power and Energy*, vol. 232, no. 7, pp. 841–855, Nov. 2018, doi: 10.1177/0957650918756761.

[16]R. Mado, A. Johanis, F. Mangngi, and I. Budayawati, "Analysis of the Effect of Double Waste Valves in Series Arrangement and Compressor Tube Layout on the Performance Efficiency of 2 Inch Hydraulic Ram Pump," in *Proceedings of the 5th International Conference on Applied Science and Technology on Engineering Science*, SCITEPRESS - Science and Technology Publications, 2022, pp. 158–163. doi: 10.5220/0011729800003575.

[17]W. Asvapoositkul, J. Juruta, N. Tabtimhin, and Y. Limpongsa, "Determination of Hydraulic Ram Pump Performance: Experimental Results," *Advances in Civil Engineering*, vol. 2019, no. 1, Jan. 2019, doi: 10.1155/2019/9702183.

[18]K. Manohar, A. A. Adeyanju, and K. Vialva, "Performance characteristics of a small water-hammer head pump," *Drink Water Eng Sci*, vol. 12, no. 2, pp. 59–64, Nov. 2019, doi: 10.5194/dwes-12-59-2019.

[19]K. Kriaa, "Effects of supply head variations on the performance of hydraulic ram pumps," *Ain Shams Engineering Journal*, vol. 16, no. 5, p. 103352, Apr. 2025, doi: 10.1016/j.asej.2025.103352.

[20]B. W. Young, "Simplified Analysis and Design of the Hydraulic Ram Pump," *Proceedings of the Institution of Mechanical Engineers, Part A: Journal of Power and Energy*, vol. 210, no. 4, pp. 295–303, Aug. 1996, doi: 10.1243/PIME_PROC_1996_210_048_02.

[21]M. Jafri, J. S. Bale, and A. R. Thei, "Experimental Study of Waste Valves and Delivery Valves Diameter Effect on the Efficiency of 3-Inch Hydraulic Ram Pumps," *International Journal of Fluid Machinery and Systems*, vol. 13, no. 3, pp. 615–622, Sep. 2020, doi: 10.5293/IJFMS.2020.13.3.615.

[22]P. J. S. Celerinos and K. D. Sanchez-Companion, "Determination of Critical Delivery Head for Hydraulic Ram Pump," *Mindanao Journal of Science and Technology*, vol. 20, no. 2, Dec. 2022, doi: 10.61310/mndjsteect.1113.22.

[23]W. Asvapoositkul, J. Juruta, N. Tabtimhin, and Y. Limpongsa, "Determination of Hydraulic Ram Pump Performance: Experimental Results," *Advances in Civil Engineering*, vol. 2019, no. 1, Jan. 2019, doi: 10.1155/2019/9702183.

[24]H. T. Dhaiban, "EXPERIMENTAL STUDY THE PERFORMANCE OF RAM WATER PUMP," *EUREKA: Physics and Engineering*, vol. 1, pp. 22–27, Jan. 2019, doi: 10.21303/2461-4262.2019.00836.

[25]M. Rahman, "Optimizing Hydraulic Ram Pump Performance: Experimental Insights on Waste Valve Height and Uncertainty Analysis," *Indian J Sci Technol*, vol. 18, no. 18, pp. 1377–1396, May 2025, doi: 10.17485/IJST/v18i18.394.

[26]G. O. Lungudi *et al.*, "Numerical and experimental analyses of hydraulic rams," *Journal of Hydraulic Research*, vol. 62, no. 5, pp. 424–440, Sep. 2024, doi: 10.1080/00221686.2024.2401899.

[27]X. Guo *et al.*, "Optimal design and performance analysis of hydraulic ram pump system," *Proceedings of the Institution of Mechanical Engineers, Part A: Journal of Power and Energy*,

vol. 232, no. 7, pp. 841–855, Nov. 2018, doi: 10.1177/0957650918756761.
[28]A. Johanis, R. Mado, and H. Dida, “Effect of Waste Valve Tuning on Hydraulic Ram Pump Efficiency,” in *Proceedings of the 4th International Conference on Applied Science and Technology on Engineering Science*, SCITEPRESS - Science and Technology Publications, 2021, pp. 237–242. doi: 10.5220/0010943000003260.
[29]M. V. de Oliveira Junior, R. T. L. da Silva, W. K. O. Moreira, J. L. de Souza, C. S. Sarmento, and J. L. dos S. Rodrigues, “PERFORMANCE OF HYDRAULIC RAM BUILT WITH DIFFERENT VOLUMES OF PVC AIR CHAMBERS,” *Revista Engenharia na Agricultura - Reveng*, vol. 29, pp. 17–27, Mar. 2021, doi: 10.13083/reveng.v29i1.10900.
[30]E. J. Schiller and P. Kahangire, “Analysis and computerized model of the automatic hydraulic ram pump,” *Canadian Journal of Civil Engineering*, vol. 11, no. 4, pp. 743–750, Dec. 1984, doi: 10.1139/l84-093.
[31]R. Fatahi-Alkouhi, B. Lashkar-Ara, and A. Keramat, “On the measurement of ram-pump power by changing in water hammer pressure wave energy,” *Ain Shams Engineering Journal*, vol. 10, no. 4, pp. 681–693, Dec. 2019, doi: 10.1016/j.asej.2019.05.001.
[32]S. Kesharwani, K. Tripura, and P. Singh, “Classical hydraulic ram pump performance in comparison with modern hydro-turbine pumps for low drive heads,” *Proceedings of the Institution of Mechanical Engineers, Part A: Journal of Power and Energy*, vol. 235, no. 6, pp. 1463–1486, Sep. 2021, doi: 10.1177/0957650921997202.
[33]M. Inthachot, S. Saehaeng, J. F. J. Max, J. Müller, and W. Spreer, “Hydraulic Ram Pumps for Irrigation in Northern Thailand,” *Agriculture and Agricultural Science Procedia*, vol. 5, pp. 107–114, 2015, doi: 10.1016/j.aaspro.2015.08.015.
[34]X. Guo *et al.*, “Optimal design and performance analysis of hydraulic ram pump system,” *Proceedings of the Institution of Mechanical Engineers, Part A: Journal of Power and Energy*, vol. 232, no. 7, pp. 841–855, Nov. 2018, doi: 10.1177/0957650918756761.
[35]W. Asvapoositkul, T. Nimitpaitoon, S. Rattanasuwan, and P. Manakitsirisuthi, “The use of hydraulic ram pump for increasing pump head-technical feasibility,” *Engineering Reports*, vol. 3, no. 5, May 2021, doi: 10.1002/eng2.12314.
[36]P. J. S. Celerinos and K. D. Sanchez-Companion, “Determination of Critical Delivery Head for Hydraulic Ram Pump,” *Mindanao Journal of Science and Technology*, vol. 20, no. 2, Dec. 2022, doi: 10.61310/mndjsteect.1113.22.
[37]Mr. Ganesh Rakate, “EFFECT OF DIAMETER OF AIR VESSEL ON EFFICIENCY OF HYDRAULIC RAM,” *INTERNATIONAL JOURNAL OF PROGRESSIVE RESEARCH IN ENGINEERING MANAGEMENT AND SCIENCE (IJPREMS)*, vol. 03, no. 04, pp. 1099–1109, 2023, Accessed: Aug. 18, 2025. [Online]. Available: https://www.ijprems.com/uploadedfiles/paper/issue_4_april_2023/30900/final/fin_ijprems1687574518.pdf
[38]R. Fatahi-Alkouhi and B. Lashkar-Ara, “Experimental Evaluation of Effective Parameters on Characteristic Curves of Hydraulic Ram-Pumps,” *Scientia Iranica*, vol. 0, no. 0, pp. 0–0, Nov. 2017, doi: 10.24200/sci.2017.4597.
[39]N. Orhan and E. Kaya, “Modeling, prediction, and optimization of pump system efficiency: A comparative study of machine learning methods and response surface method,” *Proceedings of the Institution of Mechanical Engineers, Part A: Journal of Power and Energy*, vol. 239, no. 4, pp. 624–638, Jun. 2025, doi: 10.1177/09576509251330935.